



Høgskulen på Vestlandet

Bacheloroppgave

NAB3030

Predefinert informasjon

Startdato:	12-04-2019 09:00	Termin:	2019 VÅR
Sluttdato:	03-05-2019 14:00	Vurderingsform:	Norsk 6-trinns skala (A-F + Bestått)
Eksamensform:	Prosjektoppgave		
SIS-kode:	203 NAB3030 1 PRO-1 2019 VÅR Haugesund		
Intern sensor:	(Anonymisert)		

Deltaker

Kandidatnr.: 123

Informasjon fra deltaker

Tittel *:	A case study of Flettner rotors on a fjord crossing ferry in Norway		
Engelsk tittel *:	A case study of Flettner rotors on a fjord crossing ferry in Norway		
Navn på veileder *:	Ria Bruenig		
Kan den anonymiserte besvarelsen brukes til undervisning?:	Nei	Egenerklæring *:	Ja
Jeg bekrefter at jeg har registrert oppgavetittelen på norsk og engelsk i StudentWeb og vet at denne vil stå på vitnemålet mitt *:	Ja	Inneholder besvarelsen konfidensiell materiale?:	Nei

Gruppe

Gruppenavn: (Anonymisert)
Gruppenummer: 7
Andre medlemmer i gruppen: 100, 126, 107

Jeg godkjenner avtalen om publisering av bacheloroppgaven min *

Ja



Western Norway
University of
Applied Sciences

BACHELOR'S THESIS

A case study of Flettner rotors on a fjord
crossing ferry in Norway

Jørgen Schmidt Eielsen
Kornelius Teigen Moan
Line Beate Bubandt Stenberg
Torstein Virkesdal

Nautical science

Haugesund/Western Norway University of Applied
Sciences

Supervisor: Ria Bruenig

We confirm that the work is self-prepared and that references/source references to all sources used in the work are provided,
cf. Regulation relating to academic studies and examinations at the Western Norway University of Applied Sciences (HVL),
§ 10.

Preface

The process of writing this Bachelor thesis has been very interesting and eye-opening. The task at hand turned out to be much more demanding and time consuming than first anticipated, but it has at the same time been very rewarding. During the course of our work we benefited from the many aspects in which this Bachelor program educates; navigation, stability, maritime law, mathematics, physics, metrology, green shipping, maritime English, methodology and more. The gathering of information for this study gave us new insights in wind based propulsion systems and raised our awareness about what impact the burning of fossil fuels has on the climate.

We want to show our sincerest gratitude for all the help and council provided by external actors.

Norsepower / Ville Paakkari

Norled, M/F “Oppedal” / Inger Lise Knutsen

Fjord 1 / Tor Vidar Kittang

University of applied sciences Emden-Leer / Michael Vahs - Professor in Green Shipping

Special thanks to supervisor Ria Bruenig for being there every step of the way and pointing us in the right direction. She has been a great overseer and were key in developing the calculator that made it possible to solve our thesis statement in Mathcad.

Abravission glossary

WORD/ ABBREVIATION	DESCRIPTION
CAT	Climate Action Tracker
IMO	International Maritime Organization
IPCC	The Intergovernmental Panel on Climate Change
NDC	Nationally Determined Contribution
NMA	Norwegian Maritime Authority
NNT	Norwegian National Transportation Plan
SOLAS	Safety of Life at Sea
UNFCCC	United Nations Framework Convention on Climate Change

Calculation glossary

ABBREVIATION	DESCRIPTION
Ap	Projected area
AWD	Apparent wind direction
AWS	Apparent wind speed
Beta β	Angle between course and R_w
deg	Degrees
Cd	Drag coefficient
Cl	Lift coefficient
co	Course
d	Diameter
Fd	Drag force
Fl	Lift Force
FID	Lift Force Direction
Fr	Resultant Force
FR	Flettner Rotor

ABBREVIATION	DESCRIPTION
Gamma γ	Angle between R_w and T_w
GM	Metacentric height
GZ	Righting Arm
h	Height
j	Matrix for number of different RPM cases
KG	Distance from Keel to Center of Gravity
KMt	Distance from Keel to transverse metacentre
KY	Value calculated and tabulated in the loading manual by the ship-builder from the ship's cross-curves
Lambda λ	Ratio between rotating speed of the FR and AWS
MaxT	Maximum Thrust
r	Rotated for calculation purposes
RPM	Revolutions per minute
rw	Relative Wind Direction
ss	Ship Speed
T	Thrust
tw	True Wind Direction
VCG	Vertical center of gravity (distance from keel to center of gravity)
wd	Defining wind direction from Starboard or Port side
ws	Wind speed
z	Matrix for number of different wind directions
'	Calculation purposes

Figure list

Figure 1: Fjord 1 ferry with Flettner rotors (Fjord 1 ASA)	2
Figure 2: E39 trough south and western Norway, with all the ferry routes (Staten vegvesen)	6
Figure 3: Wind flow passes a non-spinning object.....	9
Figure 4: Wind flow passes a spinning object	10
Figure 5: Lavik-Oppedal route location (Norgeskart).....	17
Figure 6: Wind speed graph	19
Figure 7: Wind rose	20
Figure 8: Flettner rotor favourable wind directions (Fjord 1 ASA).....	20
Figure 9: M/F Oppedal with Flettner rotors (Norsepower Oy Ltd.)	22
Figure 10: Flettner rotors impact on visibility	23
Figure 11: GZ curve for light ship	27
Figure 12: GZ curve for fully loaded ship.....	27
Figure 13: Polar plot	28
Figure 14: Visualization of apparent wind, true wind and relative wind	31
Figure 15: Fixed system.....	32
Figure 16: Lift and drag graph	36
Figure 17: Flettner rotor force illustration	37
Figure 18: Lavik-Oppedal route location with wind rose	45

Table list

Table 1: Fuel data form M/F Oppedal (Norled AS).....	21
Table 2: Stability requirements	26
Table 3: Final calculations	41
Table 4: Visibility and stability results	42
Table 5: Result of Flettner rotor instalment	42

Summary

This paper is a scientific study of an old invention named Flettner rotor that was proven to work as early as 1925, but discarded in favour of other cheaper alternatives available at the time. It is a rotating cylindrical sail that works by the principle of the Magnus effect to create thrust on a vessel and is much more efficient than a conventional sail design. By using it in combination with other propulsion systems it can lower the total energy consumption of a vessel considerably. The necessity for such new technological solutions in the future will be briefly explained with special regards to international climate treaties signed by Norway. A case study has been conducted on M/F “Oppedal” operating the route Lavik-Oppedal to examine whether the installation of two such sails on this ferry could be economical and technical feasible to lower the CO₂ emissions.

The result concluded that the installation of the Flettner rotors was technically possible and would reduce total amount of fuel consumption on this particular ferry by 6,1 %, equivalent to 180 tonnes of CO₂ yearly. Preventing the 180 tonnes of CO₂ from reaching the atmosphere is positive, but the down time payment of the investment was calculated to be approximately 17 years and the feasibility was therefore questioned. However rising fuel prices can in combination with cheaper rotor prices due to further development, shorten the down time payment considerably.

Sammendrag

Denne oppgaven er en vitenskapelig studie av en gammel oppfinnelse kalt Flettner rotor som ble bevist til å fungere så tidlig som i 1925, men ble forkastet til fordel for andre billigere alternativer tilgjengelig på denne tiden. Det er et roterende sylindrisk seil som fungerer på prinsippene om Magnus effekten for å lage framdrift på et skip og er mye mer effektivt enn et konvensjonelt seildesign. Ved å bruke det i kombinasjon med andre fremdriftssystemer kan det minske det totale energiforbruket til et fartøy betraktelig. Nødvendigheten av slike nye teknologiske løsninger i framtiden vil bli kort forklart med spesielt hensyn til internasjonale klima konvensjoner signert av Norge. En casestudie har blitt gjennomført på M/F "Oppedal" som driftes på sambandet Lavik- Oppedal for å undersøke om installasjonen av to slike seil på denne fergen kan være økonomisk og teknisk gjennomførbart for å minske det totale utslippet av CO₂ gasser.

Resultatet konkluderte med at installasjonen av Flettner rotorene var teknisk mulig og ville redusere totalt forbruk av drivstoff med 6,1 %, tilsvarende 180 tonn CO₂ årlig. Å forhindre 180 tonn med CO₂ fra å nå atmosfæren er positivt, men nedbetalingstiden på investeringen ble kalkulert til å være over 17 år og det ble derfor stilt spørsmål til gjennomførbarheten. Likevel kan stigende drivstoffpriser i kombinasjon med lavere priser på rotorene som følge av videreutvikling, korte nedbetalingstiden betraktelig.

Table of content

Preface.....	ii
Abravission glossary	iii
Calculation glossary	iii
Figure list.....	v
Table list.....	v
Summary	vi
Sammendrag.....	vii
1. Introduction	1
1.1 Presentation of the thesis statement.....	2
1.2 The Paris Agreement	3
1.3 Special Report.....	4
1.4 Norway and NDC	5
1.5 Ferry free E39	5
2. Theoretical basis.....	7
2.1 Wind	7
2.2 Wind as a propulsion system	7
2.3 Anton Flettner	8
2.4 The Magnus effect.....	9
2.5 Basic principle of the Flettner Rotor	10
2.6 The first rotor ship Buckau	11
2.7 Status in the modern society.....	12
2.8 Flettner Rotor operations.....	13
3. Methodology	14
3.1 Case Study	14
3.2 Choice of route	14
3.3 Choice of ferry	15
3.4 Choice of Flettner Rotor	15
3.5 Visibility requirements according to SOLAS	16
3.6 Stability requirements according to IMO and NMA.....	16
3.7 Effective thrust from the Flettner Rotors.....	16
3.7.1 Meteorological data	17

3.7.2 Fuel data	17
3.7.3 PTC Mathcad Express Prime 5.0.0.0	18
3.7.4 Theoretical vs actual effect of the Flettner Rotor	18
4. Case study M/F “Oppedal”	19
4.1 Introduction to the case study	19
4.2 The route Lavik - Oppedal	19
4.2.1 Wind data for this route	19
4.3 M/F “Oppedal”	20
4.3.1 Fuel Data for M/F Oppedal	21
4.4 Norsepower Oy Ltd	22
4.4.1 Provided assessment of installation cost	22
4.5 Calculation of blind sector created from the rotors	23
4.6 Calculation the code of intact stability	24
4.6.1 Approach for calculations	26
4.7 Calculation of thrust from the Flettner Rotor	28
4.7.1 Input values	29
4.7.2 Wind calculations	30
4.7.3 Calculations for the lift and drag graph	34
4.7.4 Force calculation	37
4.7.5 Main calculation	39
5. Results	42
6. Discussion	43
6.1 Answering the thesis statement	43
6.2 Hypothesis	44
6.3 Comparing the result with other cases	44
6.4 Actual effect VS Theoretical effect	45
6.5 Mean wind	45
6.6 Takle’s location compared to the route	45
6.7 Increase in CO2 tax	46
7. Conclusion	47
Sources	48
Attachments	53
Attachment 1. Stability calculations	53
Attachment 2. Polar plot	55

Attachment 3. Lift and drag graph	56
Attachment 4. Wind data	58
Attachment 4.1.....	58
Attachment 4.2.....	60
Attachment 5. Flettner rotor efficiency in kN	61
Attachment 6. Lavik – Oppedal timetable.....	65
Attachment 7. Specification sheet provided by Norsepower	66

1. Introduction

The following is a translated statement given by former prime minister of Norway Kåre Willoch, during an interview by host Anne Grosvold while discussing climate politics (Arendalsuka, 2018, 12:38).

This is an admonition to the one who still will not face reality.

I want to ask you: Do you think your house will catch on fire?

The answer is no.

But you still obtain insurance against fires?

Yes, of course.

This is how it is with climate politics.

*If there is a risk that humans are affecting the climate,
then this risk is so fatal that we are obliged to do what we can.*

*Then we will discover that an effective climate politic
costs a fraction compared to the damages we risk creating,
if we do not run an effective and a little costly climate politic.*

Kåre Willoch served as the Norwegian minister of trade during the 1960's and prime minister during the 1980's, an era in which the foundations of the future welfare state was created through the government's commitment to extract fossil fuel from the seafloor. The scientific consensus on how the use of fossil fuels were affecting the climate was scarce at the time. He quickly rose to become one of several key political figures that would shape the Norwegian petroleum industry development and growth towards the 21th century.

However since then Kåre Willoch, now in his 90's, has radically changed his former views on the production and use of fossil fuel as illustrated in his recent statement above. His change of heart is a result of the negative effects on the world's climate, increasingly associated with the industry due to a more established scientific consensus on the issue. The reason for discussing this is because much like Kåre Willoch, the rest of the world are becoming increasingly aware of the problems related with the production and burning of fossil fuel.

1.1 Presentation of the thesis statement

Inspired by the 16-year-old Swedish climate activist Greta Thunberg, thousands of Norwegian children and youths took to the streets on Friday 22nd of March this year to strike for the climate (Wåge, 2019). Younger generations all over the world have participated in the movement, receiving both positive and negative reactions from the rest of the world community. They demand political action from the government to drastically reduce the emissions of greenhouse gasses in the future, to be more in accordance with international climate conventions and stop the warming of the planet. Political action is very important if things are going to change, but so is also the development of technology and solutions required to make this transition. Marine shipping is estimated to be accountable for approximately 2,2 % of global CO₂ emissions (Freese, 2017, p. 3). Though the world ship owners cannot instruct all their vessels to make berth tomorrow just for the better sake of the planet, they require technological solutions making shipping more environmental friendly. The real challenge is to find a solution that can be beneficial for both the planet and the ship owners. In such a way, the thesis statement for this paper was clear:



Figure 1: Fjord 1 ferry with Flettner rotors (Fjord 1 ASA)

Source: Tor Vidar Kittang, Personal Communication, 08. November 2018

Can Flettner rotor be a feasible technical solution for ferries in Norway as a means to reach a lower environmental impact?

The Flettner Rotor is a wind based propulsions system that consist of a cylindrical rotating sail that can be mounted on any vessel. It utilizes the *Magnus effect* to create thrust through aerodynamic forces and is highly more efficient than a conventional sail design (Martin, 1926). The creation of thrust is optimal when the wind hits the side of the vessel, preferably closest to 90°. Ferries usually cross something such as a canal or a fjord, this is especially the case in Norway were the western coastline is riddled with piercing fjords. The

fjords topography will in most cases divert the wind in such a way that the optimal conditions for the Flettner Rotor will be met more often than not. The hypothesis is that by conducting a case study on a particular fjord crossing ferry route and reach the conclusion that it is feasible or not, then it could apply for the many other fjord crossings all along the coastline with similar conditions.

The word feasible in the thesis statement is a complex term defined by two factors: technical possibility according to rules of visibility and stability, but also the fuel saved compared to the cost of the investment. We have named this down time payment and it is the expected time until the cost of the investment is paid back based on how much one can save each year. Furthermore, the amount of CO₂ emission saved will be taken into special consideration. The case study contains calculation of thrust made by two Flettner Rotors installed on the vessel M/F “Oppedal”, a ferry operating between Lavik and Oppedal, in different wind conditions throughout the year. The result of the calculated thrust will be used to evaluate how much power can be reduced on the main propulsion system and therefore how much fuel can be saved and CO₂ emission reduced. This paper will first of all shortly examine how current Norwegian climate politics are in accordance with the international climate treaties undertaken by Norway. Continuing on, the theoretical basis and method for this case study will be explained before the actual case study with its coherent calculations, results, discussion and conclusion will bring this paper to an end.

1.2 The Paris Agreement

The Paris Agreement is a global reaching treaty within the *United Nations Framework Convention on Climate Change* UNFCCC aimed to limit the rise in global temperature this century. It was created during 2015 in the wake of previous conventions such as the 1992 Kyoto Protocol and 2009 Copenhagen Climate accord. They were deemed rather unsuccessful and ineffective due to their inability to unite both major and small emission contributors in the common cause to reduce the world’s emissions (Falkner, 2016).

The new climate convention goes by a different approach and does not try to distribute the total mitigation efforts among the different parties to the convention. Instead it only defines an overall objective for all the parties to reach as stated in the agreement article 2 (a) “Holding the increase in the global average temperature to well below 2°C above pre-

industrial levels and pursuing efforts to limit the temperature increase to 1.5°C above pre-industrial levels...” (United Nations, 2015, p. 3) The idea is to set aside the distributional conflict that arose among different parties in the previous conventions, by alternatively letting each individual country decide their own contribution by choice through what they call *National Determined Contributions* or NDC’s. These are documentation from each party that outline and define post 2020 actions contributing to lower emissions in the future. The first one shall be submitted by all parties until 2020 and thereafter every 5 years were every new NDC is required to exceed the goals of the previous one.

The intention is instead of demanding a certain given contribution from each party to the convention, the convention creates a unity among parties to contribute as much and as boldly as they can compared to previous commitments. As a part of the agreement, UNFCCC invited *The Intergovernmental Panel on Climate Change* IPCC to provide a special report during the year 2018 to study the impacts of global warming of 1.5°C above pre-industrial levels and related global greenhouse gas emission pathways.

1.3 Special Report

The IPCC *Special Report on Global Warming of 1.5°C* is a document released in 2018 that investigates both the effects of global warming on the environment and the possibilities to limiting any further warming of 1.5 and 2°C. Half a degree difference may not intuitively seem significant, but it is the findings of the report that the difference of limiting the global temperature between 1.5 and 2°C are quite substantial: “[...] Limiting global warming to 1.5°C is projected to reduce risk to marine biodiversity, fisheries, and ecosystems, and their function and services to humans” (IPCC, 2019, p. 10). The ocean temperature is closely linked to the global temperature. This is important as an increase in the ocean temperature will result in general increased in levels of acidity and a decrease in oxygen levels, two vital factors for the existence of marine organism. It is predicted that limiting the warming to 1.5°C will result in a 70-90% decline by the world’s coral reef, while half a degree warmer will probably end in more than a 99% decline (IPCC, 2019, p. 10). Keep in mind that coral reef support more than 25% of all species in the oceans (World Wide Fund for Nature, n.d.). A series of pathways for limiting the global rise in temperature by 1.5°C compared to pre-industrial levels illustrates it is possible, but it would require an unprecedented “never seen

before” effort and cooperation from the world community in the years to come. The way of monitoring the progress for each country in reaching this goal is through what we mentioned earlier, National Determined Contributions or NDC. An overview of each individual country and the world’s total effort can be found at *Climate Action Tracker* or CAT (Climate Action Tracker, n.d.a).

1.4 Norway and NDC

Climate Action Tracker is an independent website run by 3 different scientific organisations that review all the world countries NDC and categorize each country after how in accord they are with the new climate goal set by the Paris Agreement. The commitments are rated in such a way that if all the countries would match the contributions, then the temperature would in turn rise “that” much. For example, Norway is in the “insufficient” category where if all the world countries were to match our current contribution it would result in a warming over 2°C and up to 3°C (Climate Action Tracker, n.d.b). In reality this means that Norway’s current policies are not consistent with the goal set forth in the Paris Agreement.

A large part of Norway’s total climate effort is made by the state. The government funds projects and new development of technologies because of the benefits related, and in order to reach international climate treaties such as the one set forth in the Paris Agreement. One of these stately funded projects is the *Ferry free E39* announced forth by the Stoltenberg II government in the *Norwegian National Transportation NNT Plan* from 2013 (Samferdselsdepartementet, 2013).

1.5 Ferry free E39

European Route E39 is an approximately 1100 km stretch of coastal road running through 6 different counties from Kristiansand at the southern tip of Norway to Trondheim located in the middle. It consists of 7 different ferry connections and takes about 21 hours to

complete this present day (Statens vegvesen, n.d.)

The Stoltenberg II Government outlined in their NNT of 2013 that during the course of 20 years they wanted to connect the western part of Norway through an upgraded and ferry free E39 (Samferdselsdepartementet, 2013, p. 53), reducing total travelling time by about half. The completion would result in a more effective transportation of people and goods across the regions, and is calculated to have half the CO₂ emissions within a period of 60 years compared to continuing operating as today with ferries (Statens Vegvesen, 2016, p. 46).

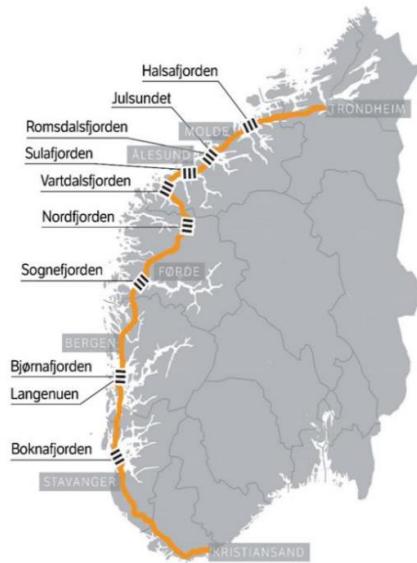


Figure 2: E39 trough south and western Norway, with all the ferry routes (Staten vegvesen)

Source: Statens vegvesen. (2016, 22. June). Ferjefri E39 – klimaeffekter. Retrieved from: <https://www.vegvesenet.no/vegprosjekter/ferjefriE39/rapportar>

A report given shortly thereafter by the Norwegian Public Roads Administration concluded that the fjord crossings was technically possible, but the provided price estimate of approximately 150 billion kroner has later almost doubled (Hope, 2019). When the Solberg government delivered their NNT of 2017 the overall plan had changed: “The Government will not connect the completion of a ferry free E39 to any specific year. The progress of realising a ferry free E39 will among other things depend on the economical flexibility and further planning, including technical solutions for the large fjord crossings:” (Samferdselsdepartementet, 2017, p. 110-111).

The longer ferry free fjord crossings comes with a very high price tag and intermediate solutions with environmentally friendly ferries operating the crossings might be part of a solution to reach the international treaties in time. This is the reason why this thesis will investigate a wind-based propulsion system with the possibility to reduce total emission of CO₂ in the years to come.

2. Theoretical basis

2.1 Wind

Wind is defined as the movement of air above the earth's surface and occurs when two masses of air with different temperature and pressure tries to reach equilibrium. The difference in temperature are responsible for the different pressures in the air. A heated mass of air will rise and create a low pressure in that region. As it rises in the atmosphere it will bend of in a direction and then be cooled again before dropping to the ground, creating a high pressure in that region. An air mass with high pressure will always move towards the air mass with low pressure and this is wind as we know it. The reason why winds tends to be stronger in the winter is because the temperature differences are greater between equator and the polar regions during this period. The difference between the cold continents and the warmer oceans is also a significant factor as to why there is more wind in the winter (Kjerstad, 2013, p. 3-96).

The direction of the wind is defined from the cardinal or intercardinal direction in which the air comes from. Wind coming from a northeast direction will be described as a north-easterly wind. The speed will normally be stated in either meters/second (m/s) or knots. The wind is rarely stable in either direction or speed, so it is common to use the average speed and direction from a 10-minute period (mean wind). If there is a limitation for which wind speed one can safely operate in, it is important to be aware of that the wind gusts can be considerably stronger than the mean wind (Kjerstad, 2013, p. 3-94).

2.2 Wind as a propulsion system

Harnessing the wind as a means of transportation can be documented as early as year 4000 BCE. The first evidence of this was found in Egypt where they constructed long trading boats to carry goods and people up and down the Nile. Some of these ships could be over 100 meters long, and used both oars and sails to navigate the river. The first sailing vessels had a rig consisting of just one square sail. A simple design that was limited to sailing in the direction of the wind and made manoeuvring very difficult. By 3000 BCE the Egyptian had begun trading with merchandise across the sea. This required a higher freeboard which made the use of oars less efficient and encouraged the development of sails. During the next centuries it was discovered that more masts could provide more sails and if designed in

different shapes and sizes, they could be controlled by sailors allowing the ships to sail up-wind. Fast forwarding to the fifteenth century when new ocean trade ways were discovered, the sailing ships greatly increase in size such as to provide more space for provision and more sails for better speed (Curley, 2011).

For thousands of years sailing ships ruled the seas as the only means of transportation, but by the beginning of the 19th century the steam engine was introduced and then later the diesel engine. The ability to move fast in any kind of weather condition with a relative cheap price tag was favoured and it marked the beginning of the end for the sailing era and wind based propulsion systems. Still there were people who saw the wind's potential:

Even in modern age of steam and electricity and gasoline engines, the wind still howls as hard as ever. As a source of driving power, the wind remains quite as available and quite as cheap as it was in the beginning of time. It still blows everywhere without cost, and it is free to anyone who will use it. (Martin, 1926)

2.3 Anton Flettner

One man that surely knew how to tame the natural forces was German inventor and aviation engineer Anton Flettner (1885-1961). During the course of his life he was responsible for numerous inventions and made important contributions to airplane-, helicopter- and ship design. Most notably of these inventions is perhaps the free-swinging-rudder, a rudder that would swing freely on its own axis with a small fin on the tip. The fin, controlled by the helmsman, is turning the rudder and thus the ship. This design required only around 5% of the power needed for turning an equally sized hinged rudder that were commonly used at the time. The new design was quickly implemented by shipbuilders for its safety- and economical advantages (Martin, 1926).

Even though the steam- and combustion engine revolutionised most of the world upon arrival, Flettner chose not to abandon wind based propulsion systems altogether. His hypothesis was that it was possible to create a greater suction power than what was possible to produce with a conventional canvas sail. He soon revolutionized years of practise in how to harness the wind, as illustrated in this quote regarding him:

It remained for the genius of Anton Flettner to reawaken us --- to prove that it is not the wind itself, but rather man's method of capturing the wind, that has run out of date.

What he has done is simply to find a new and better way. (Martin, 1926)

The new method of capturing the wind was with a cylindrical sail based on the phenomena called Magnus effect.

2.4 The Magnus effect

The Magnus effect is a term explaining what occurs when lift is created on a spinning object in fluid and was first observed in sports where spinning balls have a tendency to follow a curved path, rather than a straight line as it flies through the air. The name derives from German physicist Heinrich Gustav Magnus, the first person to experiment on the phenomena almost 170 years ago (Reid, 1997).

In order to explain how the spinning creates lift on the object, one needs to understand how air flows pass a solid surface. Fluids such as air and water have a low viscosity which means they can easily change direction and velocity of flow. Interrupting the direction of flow on a fluid with high viscosity is however much harder. Imagine pouring a bowl full of water and another bowl full of a fluid with much higher viscosity, such as maple syrup. It will be quite easy to stir the water and create a spinning flow in the bowl, but creating the same spinning flow in the bowl of maple syrup will be very hard, probably impossible. This is because fluids with low viscosity have a sticky function when it comes in contact with a solid surface (Reid, 1997). Bringing this back to the spinning object such as a ball flying through the air, the wind will deflect and flow around it. If the ball is not spinning there will not be any noticeable effect as illustrated in figure 3.

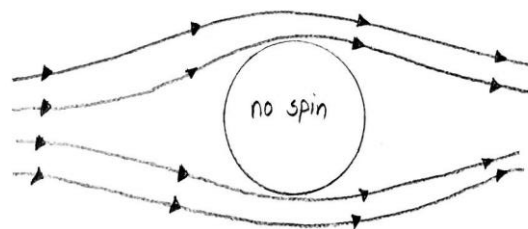


Figure 3: Wind flow passes a non-spinning object

However if the ball is spinning then the wind will bend around it quite differently. The rotating motion of the ball will drag the wind as it flows around. On the one side the wind will coincide with the direction of the spin, while on the opposite side it will be moving in the opposite direction of the spin. The air's sticky function as described before will cause the wind to accelerate on the coinciding side with low friction and decelerate at the other side with very high friction. As an equal amount of wind passes on both sides of the ball, but with a different velocity of flow, it will create a high pressure on the side with lower wind speed and a low pressure where the wind is moving faster. This is as stated in the Bernoulli's principle where the relation between speed and pressure will remain constant in a constant density of fluid. If the velocity rises then the pressure declines and vice versa (Reid, 1997). As stated previously in chapter 2.1 an air mass with high pressure will move towards the area with low pressure. The high-pressure area will create a pushing force on the ball and the low-pressure area will at the same time create a suction force on the ball (Seybold, 1925). The pushing force together with the suction force is what causes the lift, and this is what we call the Magnus effect. The lift force on the ball will push it in the direction of where the spin direction is the same as the wind direction as seen in figure 4.

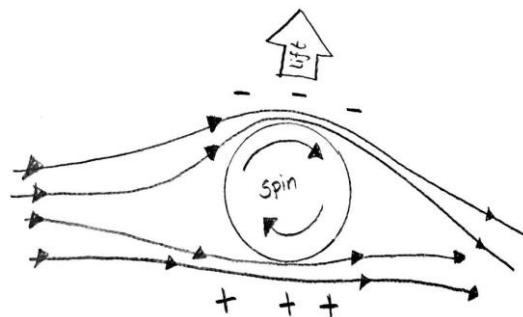


Figure 4: Wind flow passes a spinning object

2.5 Basic principle of the Flettner Rotor

The idea of Anton Flettner was to create a greater suction force than what was possible to produce with the conventional sails. Same as with the spinning ball, suction force is created from the wind accelerating around the rotor, equivalent to the air accelerated on the leeward side of the sail. Because of the rotating motion of the cylinder, the wind is accelerated with a much greater speed around the Flettner rotor than on a sail. The lifting force on the Flettner

rotor is 10 times greater than on the conventional sail of the same surface area due to the effect from the spinning. The lifting force would be created $\frac{7}{8}$ due to suction and $\frac{1}{8}$ due to pressure. (Martin, 1926). The Flettner rotors are powered by a low-voltage electrical engine, but the energy required to spin the rotors are much less compared to the thrust they produce. Data from Flettner's experiments showed that the two Flettner rotors installed on *Buckau* required approximately 10 horsepower each, to revolve at 120 rpm, and delivered together 1000 horsepower in form of thrust (Seybold, 1925).

2.6 The first rotor ship *Buckau*

In 1924 Anton Flettner's first rotors were mounted on a retired schooner called *Buckau* (Nuttall & Kaitu'u, 2016). Previously it was a sail ship, this made it easier to evaluate the effect given by the flettner rotor compared to the conventional sail rig. In the process of refitting *Buckau* he was assisted by several historical figures such as Ludwig Prandtl, Jakob Ackeret (Seifert, 2012) and Albert Einstein. Albert Einstein praised the Flettner rotor for having great practical importance (Seybold, 1925).

Buckau's maiden voyage across the North Sea in 1925 from Danzig to Scotland proved the rotor to be a much more effective alternative to conventional sails. The rotors were only one fifth of the weight compared to the old sail rig stripped away. They were able to power the vessel at speeds of up to 8 knots compared to 6,5 knots with the conventional sails. Not only was the rotor faster, lighter and required less space than the conventional sail rigs, but they also allowed the vessel to sail approximately 20 degrees closer to the wind (Gilmore, 1984). One of the more distinguishing features of a vessel equipped with a Flettner rotor, is that it will not heel like a conventional sailboat when the wind is directly from the side according to business developer at Fjord 1 Tor Vidar Kittang (Personal Communication, 08. November 2018). The reason for this is that the resulting force, acting on the rotor, is 90 degrees to the wind direction and will push on the rotor in the forward direction of the ship. As a matter of fact, sailing on a broad reach, the force vectors will cause the ship to heel into the wind rather than away from the wind (Gilmore, 1984)

2.7 Status in the modern society

The timing of Flettner's invention during the worldwide economic crisis in 1930's, known as the Great Depression, was not ideal. The newly available diesel engine was both faster and cheaper to produce. As a consequence, the idea and concept of the Flettner rotor was abandoned and "forgotten". It was not until half a century later, when the fuel prices reached a peak during the global oil crisis which started in 1973, that the idea was put back on the table. A set of German shipbuilders were planning to install a Flettner rotor on a chemical tanker, but before completion the oil prices dropped in 1986. The concept was again abandoned in favour of other technological systems (Nuttall & Kaitu'u, 2016).

Today in a period characterized by high fuel prices and environmental considerations, the Flettner rotor is starting to make its transition into the market. There are already several companies that have installed one or multiple Flettner rotors on their vessels. In 2010 Enercon completed their first commercial operation with the E-Ship 1, a specially designed vessel equipped with 4 Flettner rotors for transportation of windmill parts worldwide. In a report published in relation to the international conference on ship efficiency in 2013, Andreas Schmidt (2013a) stated that the E-Ship 1 experienced a fuel saving of 15 % overall. During favourable conditions the fuel savings could be considerably higher as the vessel was able to accomplish a speed of more than 12 knots on just the rotors alone (Schmidt, 2013a). In addition, they highlighted the vessel's good sea characteristic as the Flettner Rotors contributes to absorbing the disturbance from the sea (Schmidt, 2013b).

In April 2018 *Viking Line* equipped one of their passenger ship "Viking Grace" with a Flettner rotor delivered by *Norsepower Oy Ltd*. Build in 2013 she was already the first large passenger ship to be powered by LNG and became the first to harness the wind through a Flettner rotor. The effect given from the rotor sail will be reviewed after one year in service. Viking Line is already planning to install more rotors on their new vessel that will enter into service in 2021 (Viking Line, 2018). Norsepower has also installed Flettner rotors on the Ro/Ro ship M/V "Estraden", which according to verified measurements has saved 6,1% of its fuel consumption after the installation of the Flettner rotors. Also the installation of two Flettner rotors on the tanker Maersk Pelican is expected to reduce average fuel consumption between 7-10% (Norsepower, n.d.a).

The M/V “Afros” is an ultramax bulk carrier fitted with four Flettner rotors from *Anemoi Marine Technologies*. The rotors are fitted in such a way that they can be moved along the side of the vessel before making port, and by this arrangement minimize the risk of damage during on- and offloading operations. Anemoi is planning to install more Flettner rotors like this, to further demonstrate the technological advantages for ship owners and operators (World Maritime News, 2018).

2.8 Flettner Rotor operations

Installing the Flettner rotor on a vessel require some essential parts as described by Norsepower (n.d.b):

- Norsepower Rotor Sails, which deliver the forward thrust
- A control panel, which gives the captain full control of the operation and performance of the Norsepower Rotor Sail Solution
- A fully automatic control system, which optimises the forward thrust of the Rotor Sails
- A low-voltage electrical power supply to each Rotor Sail.

A control panel and a fully automatic control system makes the rotors user friendly for the crew. As Norsepower (n.d.b) states; it is a “push button wind propulsion” from the bridge. Andreas Schmidt (2013b) from Enercon commented that there is no extra crew required and no need for training the crew in order to be able to use the system. The fully automated Rotor-Sail system is enabled by the control system. Speed and direction of rotation is adjusted to the wind condition.

In order to keep the bearings in good condition, the rotational speed of the Flettner rotor is slowed down to idle RPM (3 RPM) every time the ship is berthing. Accelerating the Flettner rotor from idle RPM to full RPM takes less than 5 minutes (Ville Paakkari, Personal Communication, 26.02.2019).

3. Methodology

3.1 Case Study

A case study is a scientific research method used to investigate one single unit, for instance a country or a specific group of people. Jacobsen (2015, p.99) concludes that a unit within a case study will always have the common factor that they are limited in both time and space. This type of research can investigate a phenomenon thoroughly by looking into all aspects of a unit and evaluating the different parameters. Thus, drawing a detailed description and bringing a new understanding to the subject which may give life to new theories and hypothesis (Jacobsen, 2015, p.99). The case study can also be used to shed light on a topic or similar situation by being compared to other cases (Dahlum & Wæhle, 2018). However, this poses a challenge as no cases are the same. To draw a general conclusion based on one or multiple cases may not be representative for the general topic or phenomenon. Many variables are taken into consideration and other similar cases will have different variables and parameters.

To answer the thesis statement, *Can Flettner rotor be a feasible technical solution for Ferries in Norway in order to reach a lower environmental impact?*, a case study will be conducted on the ferry M/F “Oppedal” operating the route Lavik-Oppedal. The advantages of using this method in this specific case, is retaining the ability to research in detail all the different variables affecting the case and reaching a realistic result. The conclusion drawn from this may be applicable for other ferry routes operating in similar conditions. While still keeping in mind that the many different variables influencing this case, such as weather conditions, location of the rotors and fuel consumption, might differ from cases that appear similar.

3.2 Choice of route

As previously explained in chapter 2.4, wind is a fluid with low viscosity that easily changes speed and direction as it comes in contact with a solid surface. This phenomenon is also observed when wind deflects and follows the topography of a fjord where the mountain sides are steep. Considering a ferry route usually goes across a fjord, it makes sense that the wind would hit the ferry from the side for a majority of the time and therefore creating the

optimal conditions for utilizing the Flettner rotor. This case study will be conducted on the route between Lavik and Oppedal in the Sognefjord in Norway. It crosses the fjord in a north and south direction. The fjord starts at Sill by the western coast of Norway and stretches 175 km in an easterly direction to Skjolden (Svendsen, 2006). The landscape is characterized by steep mountains on each side, and the wind will follow in a westerly direction or vice versa the majority of the time.

3.3 Choice of ferry

The route Lavik-Oppedal is a part of E39 and there are three ferries operating this route on a daily basis, all belonging to Norled. M/F “Ampere” is a fully electrical ferry and so environmentally friendly that it did not make sense to conduct this case study on this vessel. M/F “Stavanger” was quickly considered to be too short in order to fulfil the visibility requirements provided by SOLAS, which will be further explained in chapter 3.5. The decision therefore landed on the 113,56 meters long M/F “Oppedal”, which is the ferry that this case study will be conducted on.

3.4 Choice of Flettner Rotor

In order to conduct the case study there was a need to specify the rotor sail location, size and how many should be installed to achieve the optimal effect for the vessel. As a rule of thumb the bigger sails make the better business case, but there are still some critical topics that should be consider beforehand. The cargo and passenger operations must still be able to continue quite smoothly on without any significant problem. In this case for example, the instillation of rotor sails in the bow and stern sections of the vessel might later turn out to be a major inconvenience during operations. The diameter of the cylinder might be limited to a certain size in order to get cars around the cylinder during on- and unloading of vehicles. Lacking the ability and knowledge to make these kinds of decisions, a company that develop and install these types of rotor sails was consulted: Norsepower. This will be further explained in chapter 4.4.

3.5 Visibility requirements according to SOLAS

Before installing any tall object on deck there is a set of visibility requirements that needs to be upheld as specified in *SOLAS Chapter V Regulation 22 Navigation Bridge Visibility* (IMO, 2014). Installing just one of these rotors in the wrong place or with the wrong height, could limit the visibility to the extent that it could possibly create dangerous situations. The SOLAS convention of 1974 specifies that each individual blind sector from the conning position should not exceed 5 degrees.

3.6 Stability requirements according to IMO and NMA

The Flettner rotors will be an external weight mounted on the deck with a high centre of gravity, which will affect the vessel total centre of gravity. Before installing the Flettner rotors on M/F “Oppedal”, the code of intact stability needs to be evaluated according to IMO’s requirements. In addition to this, M/F “Oppedal” stability sheet has some extra stability requirements listed according to the *Norwegian Maritime Authority* (NMA). The calculations on stability regarding the installation of two Flettner rotors with the centre of gravity 6 meters above the foundation is shown in attachment 1. The data for which the calculation is based upon is gathered from M/F “Oppedal” stability sheet and the specification sheet from Norsepower (Attachment 7). The IMO requirements together with the results from the calculation is presented in table 2 in chapter 4.6.

3.7 Effective thrust from the Flettner Rotors

The following will be a description of some important parameters and tools, that have been used for the thrust calculations.

3.7.1 Meteorological data

The meteorological data used for the calculations have been specially ordered for this case from Eklima. This data is accumulated at Takle weather station, located 38 meters above sea level and approximately 4-5 nautical miles southwest from the route Lavik-Oppedal as shown in figure 5. The Meteorological data is shown in attachment 4.1 and displays the mean wind speed and direction every day at 1200 noon throughout the year 2013. The reason why measurements from 2013 were used, and not from 2018 to match the fuel consumption data gathered from M/F “Oppedal”, is because the weather station stopped measuring wind data in 2014.

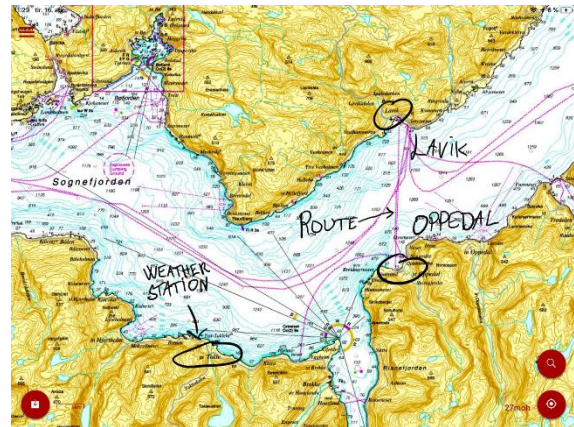


Figure 5: Lavik-Oppedal route location (Norgeskart)

Source: Norgeskart)

3.7.2 Fuel data

In order to calculate how much fuel can be saved by installing the Flettner rotors, the data for fuel consumption needs to be taken in as a factor as well as the power developed by the engine and the fuel prices. The data for the fuel consumption is gathered from M/F “Oppedal” for 2018 by consulting with Norled. We could not base our calculations of fuel consumption data from 2013 to match the wind data, simply because the ferry was not operating the route in this period. Engineer on board M/F “Oppedal”, Per Øren, has stated the power developed by the engine on the 22.04.2019 to be 800kW (Personal Communication, 22.04.2019). Regarding the fuel prices, that changes from day to day, the thesis are basing its value stated by Bunker Oil AS on the 25.04.2019 (Tore Slinning, Personal communication, 25.04.2019).

3.7.3 PTC Mathcad Express Prime 5.0.0.0

Calculating the thrust induced by the Flettner rotor on a day to day basis, created the need to consider the everyday variations in wind conditions throughout the year. It is done in the mathematical program PTC Mathcad Express Prime 5.0.0.0, to make a systematic and neat view of the whole process. Mathcad allows the user to define formulas, variables and constants in such a way that the different parameters can be inserted and the results comes out at the end of a *calculator*. The advantage of this method is that the calculator produced in this project, can be reused in a different case with other parameters. If for instance a similar case study were to be conducted on another ferry in a different location, then all the new variables this would bring about could be directly inserted and the result would be produced by the calculator. Results from all calculations done in Mathcad is shown in attachment 5. An explanation, as well as an example is shown in chapter 4.7 together with the final results.

3.7.4 Theoretical vs actual effect of the Flettner Rotor

The procedure for this study is mostly based on a calculation method thought by Professor Michael Vahs in Green Shipping (NAB 3036) at Western Norway University of Applied Sciences (Vahs, 2018). Michael Vahs is a professor with long experience in scientific studies and experiments with Flettner rotors. According to him the mathematical model of calculating the effect of the Flettner rotor will in many cases predict a lower result, than the actual effect given by the Flettner rotor during testing. He and his coworkers measured higher thrust in the range of 10-40 % in relation to the previous predictions based on model tests. They are currently studying the Reynolds Number effect on the upscaling from model testing to real size cases. The Reynolds number is a factor used to predict flow pattern in fluid mechanics. Michael Vahs explained that this still has to be proven, which he and other scientists at Emden-Leer and Delft university are currently trying to do (Vahs et al. 2019, p 12-20).

4. Case study M/F “Oppedal”

4.1 Introduction to the case study

The following chapter is a review of all data collected in order to complete this thesis and the calculations done to get the results. A description of the subject for this case study, the route Lavik-Oppedal and the ferry M/F “Oppedal”, will be introduced with the gathered data. Further in this chapter the results of the calculations regarding visibility requirements and stability requirements are presented, before moving on to a review of the calculated effect from the Flettner rotors.

4.2 The route Lavik - Oppedal

The route between Lavik and Oppedal has been operational since 1990 (NRK Sogn og Fjordane, 2002). The trip across the Sognefjord takes approximately 20 minutes and the ferries spends 10 minutes in each harbour unloading and loading. The ordinary service speed across the fjord is 10 knots. The route is a one-stretch route going south and north.

4.2.1 Wind data for this route

The wind data collected from Eklima has been arranged into two graphs to be more understandable. 9% of the wind direction have not been accounted for due to the equipment failure on the weather station. In the first graph (figure 6) the number of days throughout the year is displayed on the y-axis and the wind speed are on the x-axis. The wind speed is categorized for each 1 m/s increase.

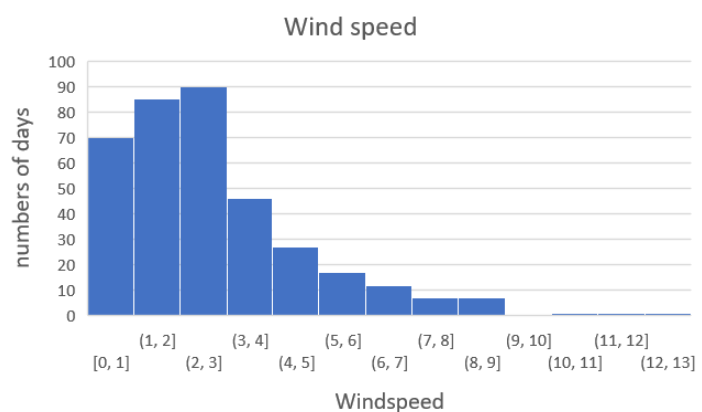


Figure 6: Wind speed graph

The second graph (figure 7) is a wind rose displaying where and how often the wind comes from any given direction during the year. The wind is split into 12 different categories and the value is in percentage. The figure gives an indication on how the wind directions are in the area. The stronger the wind the more thrust Flettner rotor could produce, but the wind has to come from a favourable direction.

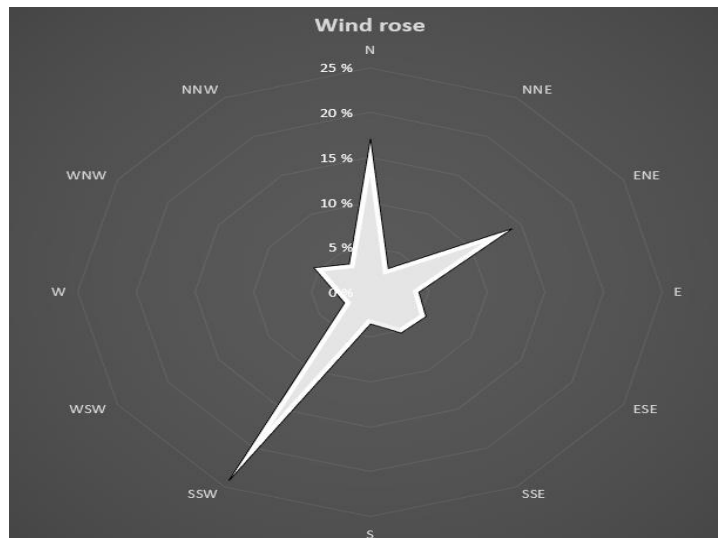


Figure 8: Wind rose

Figure 8 gives a visual representation of which wind directions the Flettner rotor can produce forwards thrust from. If the vessel is heading directly North or South, then the rotor can produce forward thrust if the wind comes from either 30°-150° or 210°-330°. The green sectors show the favourable wind directions, while the wind from the red sectors can be neglected.

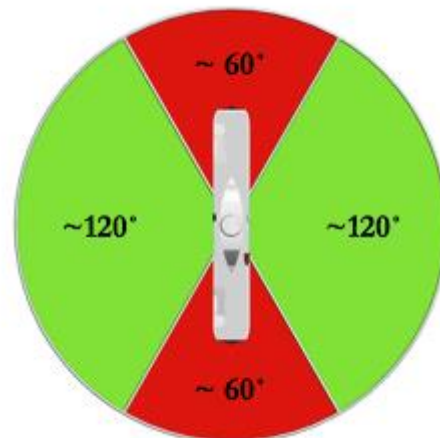


Figure 7: Flettner rotor favourable wind directions (Fjord 1 ASA)

Source: Tor Vidar Kittang, Personal Communication, 08. November 2018

4.3 M/F “Oppedal”

M/F “Oppedal”, former M/F “Tidesund”, is a diesel electric ferry build in 2008 by Fiskerstrand Verft AS. She is 113,56 meters long, 17,20 meters wide and with the capacity of 350 passengers, 120 personal vehicles and 10 trailers (Multi Maritime A/S, 2008). M/F “Oppedal” completes 46 trips between Lavik and Oppedal on ordinary weekdays, 40 trips on Saturdays and 40 trips on Sundays. This makes a total of 310 trips throughout the week (Norled, 2018). She is propelled by four Mitsubishi diesel engines: two larger engines of the S12R-MPTK type and two smaller of the S6R2-MTPTKF type. These have an output of respectively 1200kW and 640 kW each. Additionally there are four Stamford generators, one

pair delivering 1345 kVA and the other pair delivering 765kVA. There are two Schottel STP 1010 propellers driving the vessel forward (Skipsrevyen, 2008). The engines burn through an average of 2910 litres of marine diesel oil per day and it is this number the installation of the Flettner rotors might be able to partially reduce.

4.3.1 Fuel Data for M/F Oppedal

Table 1 display the total amount of marine diesel spent throughout the year 2018 month by month and the total amount of hours the engine was running. This table was provided by Inger Lise Knutsen, officer at Norled (Personal Communication, 04.02.2019).

Month	Total diesel consumption, per month (Litre):	Total amount of hours the engine is running per month:
January	102 000	739
February	78 680	655,5
March	102 400	741,5
April	76 592	715,5
May	108 000	733,5
June	43 191	392
July	64 002	669
August	112 567	711,5
September	96 069	693,5
October	94 234	717,5
November	90 619	708
December	93 637	733,5

Table 1: Fuel data form M/F Oppedal (Norled AS)

M/F “Oppedal” consumed a total of 1 061 991 litres of marine diesel during the year of 2018. By dividing this number with the number of days in a year (365), the average fuel consumption per day is 2910 litres. The total amount of hours the engine was running in 2018 was 8210 hours, which means that the engine spends an average of 129 litres per hour (1061991 litres/8210 hours). Fuel prices received on 25.04.2019 from Bunker Oil AS was 4,73 Norwegian kroners per litre. This price varies from day to day. In addition, the ferries need to pay CO₂ taxes. The CO₂ taxes are set in the state budget and are regulated every year. The CO₂ taxes in 2019 is 1,35 Norwegian kroners per litre, and this number is increasing every year. Since last year the CO₂ taxes have increased with 0,02 Norwegian kroners, according to Tore Slinning, sales manager in the marine section of Bunker Oil AS (personal communication, 25.04.2019)

4.4 Norsepower Oy Ltd.

Norsepower is a leading company in the market for auxiliary wind propulsion system with the goal of reducing the environmental impact of marine shipping. Since their start up in late 2012 they have installed Flettner Rotor on a variety of ships such as the ro-ro vessel M/V “Estraden” and the cruise ferry M/S “Viking Grace”. They were willing to provide their expertise and suggested that two rotors with the dimensions 3x18m mounted 35 meters from the bridge would be the optimal setup for M/F “Oppedal” as illustrated in the figure 9:

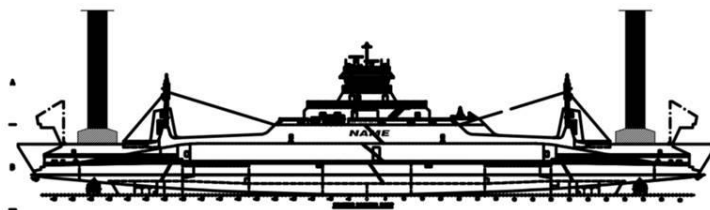


Figure 9: M/F Oppedal with Flettner rotors (Norsepower Oy Ltd.)

Source: Ville Paakkari, Personal Communication, 08. April 2019

4.4.1 Provided assessment of installation cost

Norsepower provided “ball park prices” for their rotors with the smallest dimensions. 3x18m cost 300 000 euros per unit and 50 000 euros for the installation per unit (Ville

Paakkari, Personal Communication, 12. March 2019). The price for the installation all together will then be $2 \times (300\,000 \text{ euros} + 50\,000 \text{ euros}) = 700\,000 \text{ euros}$. Since fuel prices in this thesis is stated in Norwegian kroners, the price of the rotor installation needed to be converted in to Norwegian kroners. For this the currency from Norges Bank on the 25. April 2019 were used. The currency for this date was 1 EUR = 9,6638 Norwegian Kroner (Norges Bank, 2019). The price of the rotor installation in Norwegian kroner would be $(700\,000 \times 9,6638) = 6\,764\,660 \text{ kr}$.

4.5 Calculation of blind sector created from the rotors

The overall length of M/S “Oppedal” is 113,56 meters and the bridge is located at the centre of the ship (Multi Maritime A/S, 2008). The diameter of the Flettner rotors to be installed are 3 meters and they will be placed on each side of the bridge in a distance of 35 meters from it.

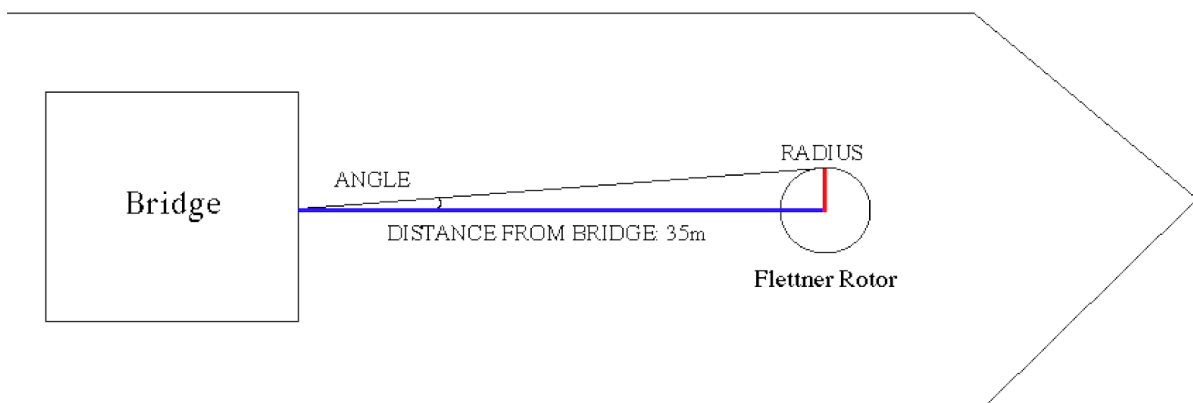


Figure 10: Flettner rotors impact on visibility

By using simple geometry half of the blind sector can be found. The rotors radius (red line in figure 10) is one cathetus, while the distance from the bridge is the other cathetus (blue line in figure 10). The rotors radius is equal to the diameter divided by 2, which is 1,5 meters. The tangent of the angle in the figure is equal to the radius divided by the distance from the bridge. Reversing this equation, the angle will be equal to the tangent inverse of the rotor’s radius divided by the distance from the bridge. Multiply it by 2 and the whole blind sector is found:

$$\text{Tan}^{-1}(1,5\text{m}/35\text{m}) * 2 = 4,9^{\circ}$$

Calculations proves indeed that the blind sector does not exceed 5° by this rotor setup, but considering the small margin of only $0,1^{\circ}$ it may be advised to locate them even further from the bridge if possible. This thesis will however keep with this setup as provided by Norsepower.

4.6 Calculation the code of intact stability

In the table below there is a list of all requirements by IMO (IS-Code, 2008, 2.2) and NMA (Forskrift om bygging av skip, 2014, §19-4), and the results from the stability calculations with the Flettner rotors;

IMO's requirements	Values for light ship	In accordance with requirements	Values for fully loaded ship	In accordance with requirements
The area under the GZ-curve from 0° to 30° shall not be less than 0,055 metre-radians	0,777 metre-radians	YES	0,625 metre-radians	YES
The area under the GZ-curve from 0° to 40° shall not be less than 0,09 metre-radians	1,155 metre-radians	YES	0,850 metre-radians	YES
The area under the GZ-curve from 30° to 40° shall not be less than 0,03 metre-radians	0,377 metre-radians	YES	0,225 metre-radians	YES
The GZ should be at least 0,20 m at an angle of heel equal to, or greater than 30°	2,321 metre-radians	YES	1,551 metre-radians	YES

IMO's requirements	Values for light ship	In accordance with requirements	Values for fully loaded ship	In accordance with requirements
The maximum GZ shall occur at an angle of heel not less than 25°	Maximum GZ is between 25° and 30°	YES	Maximum GZ is between 20° and 25°	NO
The initial Metacentric height, GM, should not be less than 0,15 meters	6,372 meter	YES	5,512 meter	YES
The angle of heel on account of crowding of passengers to one side should not exceed 10°	Without the rotors, this is equal to 0,9° Assuming the rotors won't have any large effect on this angle, it will not exceed 10° with the rotors.	YES	Without the rotors, this is equal to 0,9° Assuming the rotors won't have any large effect on this angle, it will not exceed 10° with the rotors.	YES
Requirements as specified by NMA				
The area under the GZ-curve from 0° to 20° shall not be less than 0,055 metre-radians	0,382 metre-radians	YES	0,332 metre-radians	YES
Maximum GZ shall be at least twice as high as the GZ of the angle of heel when half of the vehicles	$GZ_{MAX} \approx 2,32 > 2 * GZ_{5^\circ}$	YES	$GZ_{MAX} \approx 1,71 > 2 * GZ_{5^\circ}$	YES

IMO's requirements	Values for light ship	In accordance with requirements	Values for fully loaded ship	In accordance with requirements
the ferries can carry are placed on one side.				

Table 2: Stability requirements

4.6.1 Approach for calculations

Attachment 1 shows the calculations for the new GZ-curve both in light ship condition and in fully loaded condition with the two Flettner rotors installed on deck. The specifications for the light ship and fully loaded condition of M/F "Oppedal" can be found in the stability sheet for M/F "Oppedal". Information about the Flettner rotors is retrieved from Norsepower's technical specification sheet that can be found in attachment 7, where the weight of the Flettner rotor and foundation together is 29 tonnes. The rotors centre of gravity is located 6 meters above the foundation (Ville Paakkari, personal communication, 16.04.2019) and the foundation is 2 meters high, so the KG for the Rotors would be 8 meters above the deck. The distance from the keel to the deck is 5,5 meters, so the initial KG for the rotors will be 13,5 meters. The KY values are retrieved from the table in chapter 6 in the stability sheet and the necessary intermediate values have been found by linear interpolation. The same process is repeated with the value of KMt taken from the table in chapter 5 in the stability sheet (Multi Maritime A/S, 2008).

The installation of two Flettner rotors resulted in the following GZ curve for light ship condition in figure 11 and fully loaded condition in figure 12.

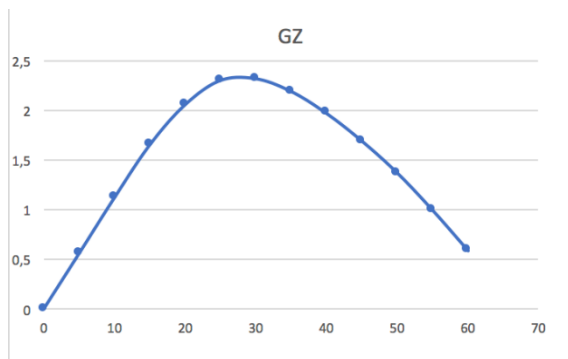


Figure 11: GZ curve for light ship

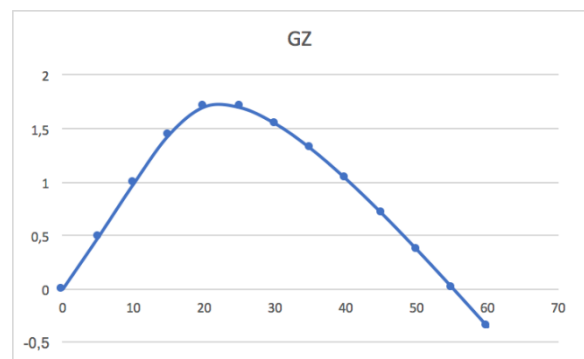


Figure 12: GZ curve for fully loaded ship

From these graphs it was possible to calculate the respective areas under the curve by using the Simpson's formula. The areas under the GZ-curve are in accordance with the requirements in both light ship- and fully loaded condition. However, if the vessel is to follow IMO's requirements for intact stability some small adjustments are needed if the maximum GZ shall occur above 25 degrees in fully loaded conditions. Another alternative criteria can be made and approved by the Administration based on an equivalent level of safety according to the adoption on the international code on intact stability (IS-Code, 2008, 2.2.3).

One requirement by NMA states the maximum GZ shall be twice the GZ value occurring at the angle of heel, when half the weight of all vehicles that the ferry is certified to carry are placed on one side. In the stability sheet this angle of heel is stated to be somewhere between 3,12 and 3,68 degrees. For practical reasons the value for GZ at an angle of 5 degrees were used and resulted in a maximum GZ in accordance with the requirement.

Calculation of the new GM based on the new values for KM_t and KG with the Flettner rotors installed proved that the new initial metacentric height is well above IMO and the NMA requirements:

$$\begin{aligned}
 \text{Light ship: } & GM = KM_t - KG & GM = 12,123m - 5,751m = 6,372m \\
 \text{Fully loaded ship: } & GM = KM_t - KG & GM = 11,565m - 6,053m = 5,512m
 \end{aligned}$$

Lastly there is a requirement stating that the vessel shall not have an angle of heel exceeding 10° when all the passengers are placed on one side. In the stability sheet the angle

of heel with all the passengers placed on the port side is stated to be $0,9^\circ$. The Flettner rotors have affected the stability in all conditions to a very small extent and it is very unlikely that the installation will increase the angle by $9,1^\circ$. The assumption is therefore that this value will be in accordance with the requirement.

4.7 Calculation of thrust from the Flettner Rotor

Figure 13 is the polar plot based on the results in Attachment 2. The polar plot illustrates the amount of power produced by one Flettner rotor in different wind conditions. In the calculator described in this chapter, the polar plot is made by inserting all values for wind speed from 1-15 m/s and all the wind directions illustrated in the green sector in figure 8. The “circles” in the polar plot represents the amount of kN that is produced by one rotor, in the different wind directions. The coloured lines represent the different wind speeds in m/s. For example, wind from 250° with wind speed of 15m/s produces close to 45 kN of thrust from the Flettner rotor.

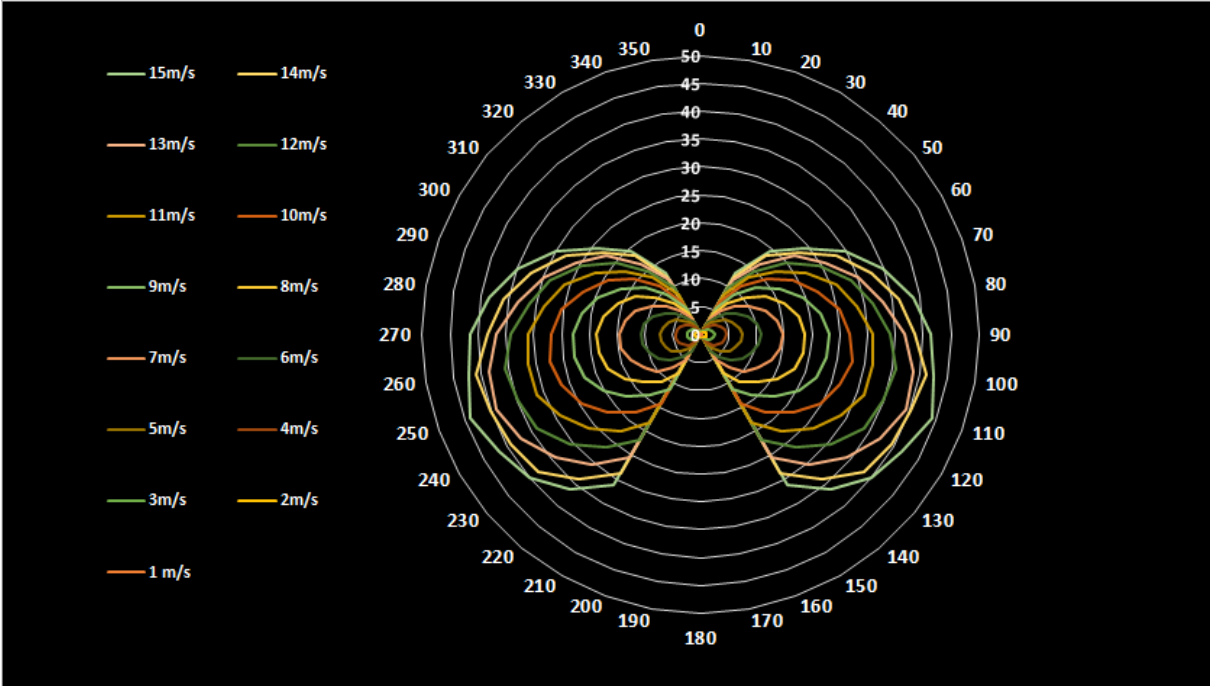
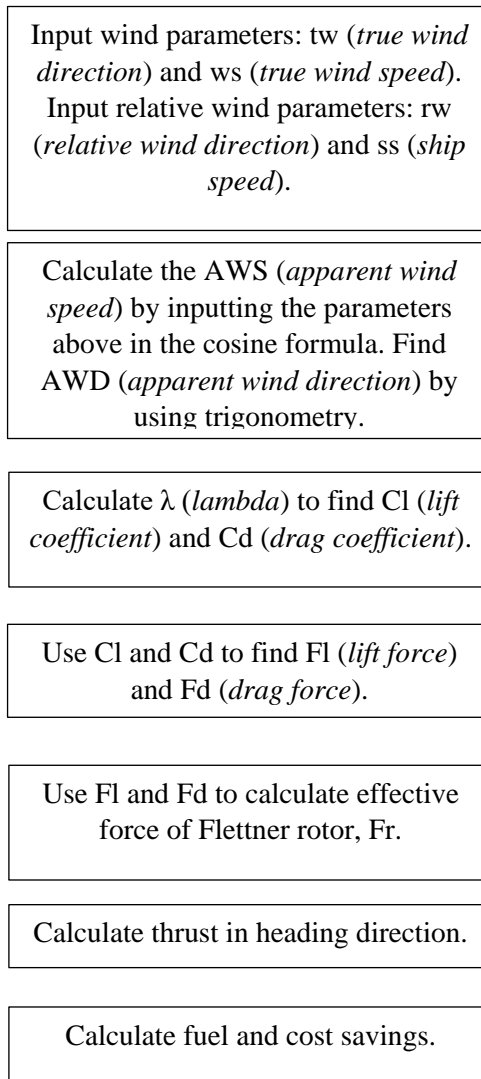


Figure 13: Polar plot

In the calculations below, an example is presented showing step by step how the Mathcad “calculator” works. Four different wind conditions and two different courses are used in this example. Each formula is preceded by an explanation. Certain matrices are

shortened due to the many numbers the calculations produce and for the sake of simplicity some intermediate results will only be shown with an indication of the numbers.

Furthermore, the calculations done in this thesis are in the same manners as these examples and follows the order illustrated by the flow chart below.



4.7.1 Input values

The input values define the constants and variables. The different input values can be changed for any scenarios. This makes the calculator possible to use in other cases, where the

input values would just need to be redefined. The following input values are defined for M/F “Oppedal” case study. These values will also be used for the examples later.

j defines the number of different RPMs the calculator will use, in this example the RPM starts at 10 and increases with an interval of 10 up to 230 RPM. This makes 23 different values for j (0-22).

$$j := 0 .. 22$$

z defines the number wind directions, for this example four different wind directions are used (0-3).

$$z := 0 .. 3$$

The wind speed (ws), true wind direction (tw), the courses (co) and the speed of the ship (ss) is inserted as variables.

$$ws := 5.2 \frac{m}{s} \quad tw := \begin{bmatrix} 240 \\ 220 \\ 60 \\ 70 \end{bmatrix} deg \quad co := \begin{bmatrix} 360 \\ 180 \\ 360 \\ 180 \end{bmatrix} deg \quad ss := 5.1 \frac{m}{s}$$

The dimensions of the Flettner rotor is defined for this case.

$$d := 3 \text{ m} \quad Ap := 53.4 \text{ m}^2 \quad h := 18 \text{ m}$$

The air density is defined.

$$Rho := 1.23 \frac{kg}{m^3}$$

4.7.2 Wind calculations

True wind is the direction of the wind measured by a stationary observer. Relative wind is created by the ship moving forward through the air and will always be the opposite of the course. Apparent wind is the direction and velocity of the wind measured by an anemometer on a moving vessel. This is illustrated in figure 14.

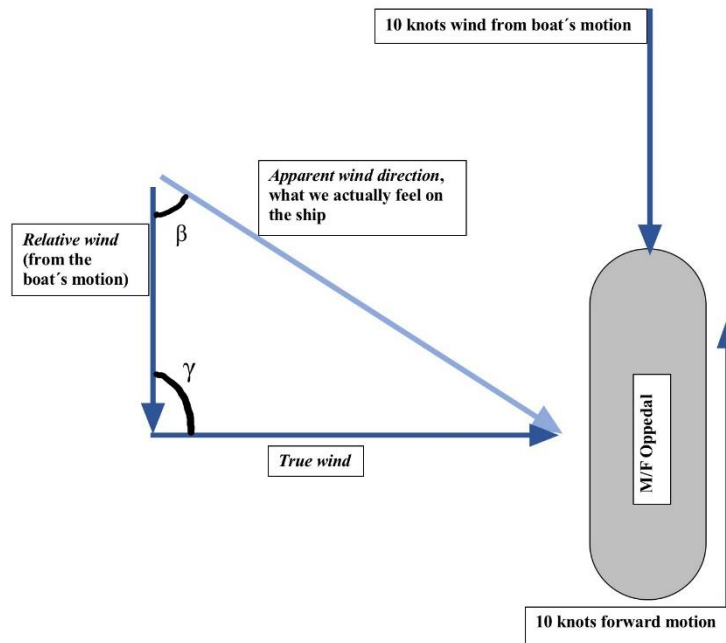


Figure 14: Visualization of apparent wind, true wind and relative wind

In this case the ship has two courses, north and south. To be able to calculate with the two courses in Mathcad, the relative and true wind directions as well as the course needs to be rotated into a fixed direction/course. For this the r is defined in order to rotate the wind directions and courses in further calculations. This is crucial for the calculations to work properly in the Mathcad calculator.

$$r := 360 \text{ deg} - co \quad r = \begin{bmatrix} 0 \\ 180 \\ 0 \\ 180 \end{bmatrix} \text{ deg}$$

In the following formulas, co_r , rw_r and tw_r , the r is used to rotate the course and winds into the fixed system. In the fixed system all the courses are rotated to 360 deg . The relative and true winds will be rotated so that the angle between the courses and winds are the same as before.

$$co_r := co + r \quad co_r = \begin{bmatrix} 360 \\ 360 \\ 360 \\ 360 \end{bmatrix} \text{ deg}$$

$$rw_r := co_r - 180 \text{ deg} \quad rw_r = \begin{bmatrix} 180 \\ 180 \\ 180 \\ 180 \end{bmatrix} \text{ deg}$$

$$tw_r := tw + r \quad tw_r = \begin{bmatrix} 240 \\ 400 \\ 60 \\ 250 \end{bmatrix} \text{ deg}$$

Figure 15 is an illustration of how the rotation would look like in the fixed system.

The fixed system

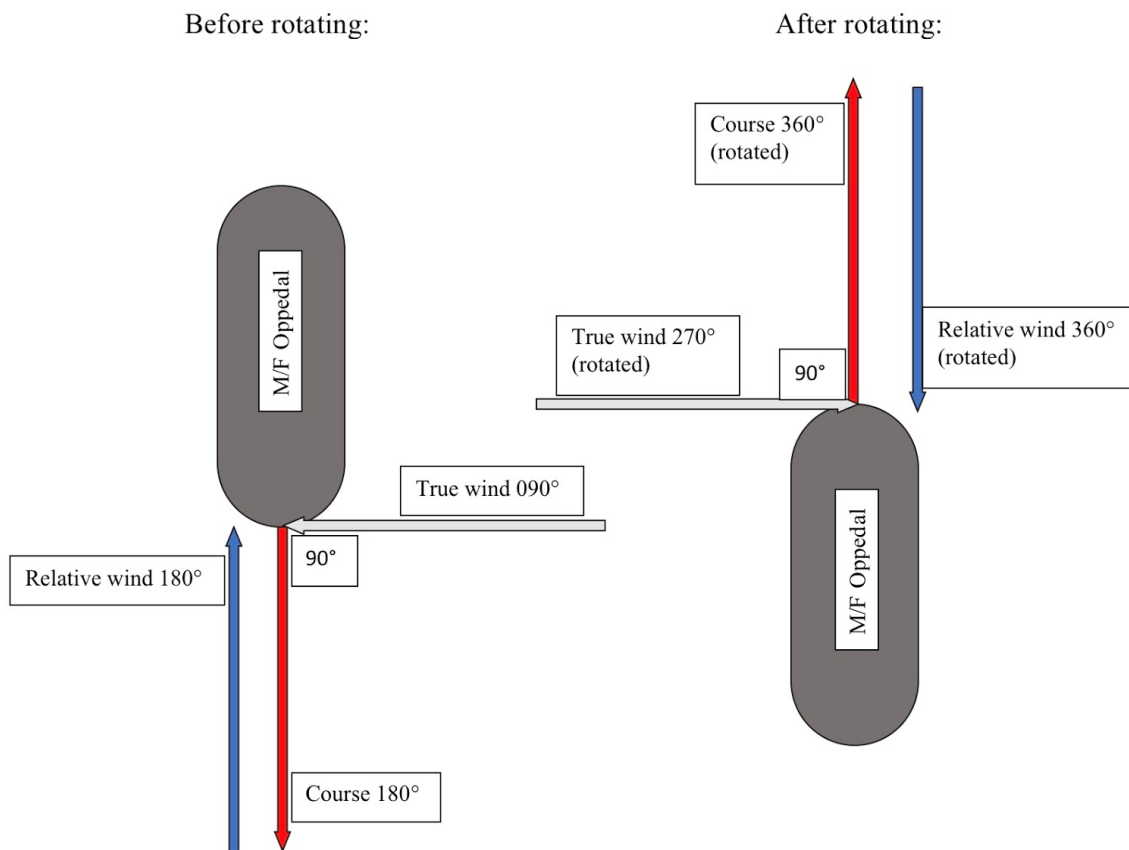


Figure 15: Fixed system

γ is the angle between the tw_r and rw_r .

$$\gamma := rw_r - tw_r \quad \gamma = \begin{bmatrix} -60 \\ -220 \\ 120 \\ -70 \end{bmatrix} \text{deg}$$

The apparent wind speed (AWS) is calculated by using the cosine formula.

$$AWS := \sqrt{ws^2 + ss^2 - 2 \cdot ws \cdot ss \cdot \cos(\gamma)} \quad AWS = \begin{bmatrix} 5.151 \\ 9.679 \\ 8.92 \\ 5.908 \end{bmatrix} \frac{m}{s}$$

β is the angle between rw and AWD and is also calculated by using the cosine formula.

$$\beta := \arccos\left(\frac{AWS^2 + ss^2 - ws^2}{2 \cdot AWS \cdot ss}\right) \quad \beta = \begin{bmatrix} 60.963 \\ 20.202 \\ 30.321 \\ 55.794 \end{bmatrix} \text{deg}$$

wd' defines if the wind is coming from port or starboard side. wd' between 000-180 deg is starboard side and wd' between 180-360 deg is port side. The function «trunc» removes all decimals.

$$wd' := tw_r - \left(\text{trunc}\left(\frac{tw_r}{361 \text{ deg}}\right) \cdot 360 \text{ deg} \right) \quad wd' = \begin{bmatrix} 240 \\ 40 \\ 60 \\ 250 \end{bmatrix} \text{deg}$$

wd defines if the angle β is added or subtracted later on in the calculations. Port (+1) will be positive and starboard (-1) will be negative.

$$wd := \frac{wd' - 180.5 \text{ deg}}{\sqrt{(wd' - 180.5 \text{ deg})^2}} \quad wd = \begin{bmatrix} 1 \\ -1 \\ -1 \\ 1 \end{bmatrix}$$

AWD' defines the apparent wind direction. This formula below also rotates the wind directions and courses back to the initial coordination system.

$$AWD' := \overrightarrow{co_r - wd \cdot \beta - r} \quad AWD' = \begin{bmatrix} 299.037 \\ 200.202 \\ 390.321 \\ 124.206 \end{bmatrix} \text{ deg}$$

AWD is redefining AWD' as a number between 000-360 deg.

$$AWD := AWD' - \left(\text{floor} \left(\frac{AWD'}{361 \text{ deg}} \right) \cdot 360 \text{ deg} \right) \quad AWD = \begin{bmatrix} 299.037 \\ 200.202 \\ 30.321 \\ 124.206 \end{bmatrix} \text{ deg}$$

4.7.3 Calculations for the lift and drag graph

The $RPM_{z,j}$ defines all the different values for rotational speed that the rotor operates in. The four rows in the matrix represents the four wind directions in this example, defined by z. The different values of $RPM_{z,j}$ depend on what number «j» is defined as. The reason for the many RPM values, is that different wind speeds requires different RPM values in order to get the most effect from the rotors. The Mathcad calculator will find the optimal RPM for any given wind speed.

$$RPM_{z,j} := (10 + 10 \cdot j) \frac{1}{\text{min}} \quad RPM = \begin{bmatrix} 10 & 20 & 30 & 40 & 50 & 60 & 70 & 80 & 90 & 100 & 110 & 120 & 130 & 140 & 150 & 160 & 170 & 180 \\ 10 & 20 & 30 & 40 & 50 & 60 & 70 & 80 & 90 & 100 & 110 & 120 & 130 & 140 & 150 & 160 & 170 & 180 \\ 10 & 20 & 30 & 40 & 50 & 60 & 70 & 80 & 90 & 100 & 110 & 120 & 130 & 140 & 150 & 160 & 170 & 180 \\ 10 & 20 & 30 & 40 & 50 & 60 & 70 & 80 & 90 & 100 & 110 & 120 & 130 & 140 & 150 & 160 & 170 & 180 & \dots \end{bmatrix} \frac{1}{\text{min}}$$

Lambda (λ) is the ratio between the rotational speed of the Flettner rotor and the apparent wind speed. This formula calculates the lambda(λ) for all the different RPM values to find the optimal lambda for each case.

$$\lambda_{z,j} := \frac{\overrightarrow{RPM_{z,j} \cdot \pi \cdot d}}{AWS_{z,0}}$$

$$\lambda = \begin{bmatrix} 0 & 1 & 2 & 3 & 4 & 5 & \dots & 22 \\ 0.305 & 0.610 & 0.915 & 1.220 & 1.525 & 1.830 & & \\ 0.162 & 0.325 & 0.487 & 0.649 & 0.811 & 0.974 & & \\ 0.176 & 0.352 & 0.528 & 0.704 & 0.880 & 1.057 & & \\ 0.266 & 0.532 & 0.798 & 1.063 & 1.329 & 1.595 & \dots & \end{bmatrix}$$

In this function lambda is rounded to the closest decimal. This is because the lambda numbers in the λ Graph are restricted to one decimal.

$$\lambda_r := \overrightarrow{\text{round}(\lambda, 1)} = \begin{bmatrix} 0.3 & 0.6 & 0.9 & 1.2 & 1.5 & 1.8 & 2.1 & 2.4 & 2.7 & 3 & 3.4 & 3.7 \\ 0.2 & 0.3 & 0.5 & 0.6 & 0.8 & 1 & 1.1 & 1.3 & 1.5 & 1.6 & 1.8 & 1.9 \\ 0.2 & 0.4 & 0.5 & 0.7 & 0.9 & 1.1 & 1.2 & 1.4 & 1.6 & 1.8 & 1.9 & 2.1 \\ 0.3 & 0.5 & 0.8 & 1.1 & 1.3 & 1.6 & 1.9 & 2.1 & 2.4 & 2.7 & 2.9 & 3.2 & \dots \end{bmatrix}$$

Figure 16 is the Cl and Cd graph. It shows the lift and drag coefficient for the given lambda (λ). This graph is based on values from Da-Quing, Leer-Andersen & Allenström. (2012). To make the graph as exact as possible in order for the Mathcad calculator to use it, the intermediate numbers in the graph have been calculated by linear interpolation. According to Rohden (2012) there is no significant difference between Cl and Cd after lambda (λ)=4. This made it possible to extend the table in attachment 3, which this graph is based upon, for calculation purposes.

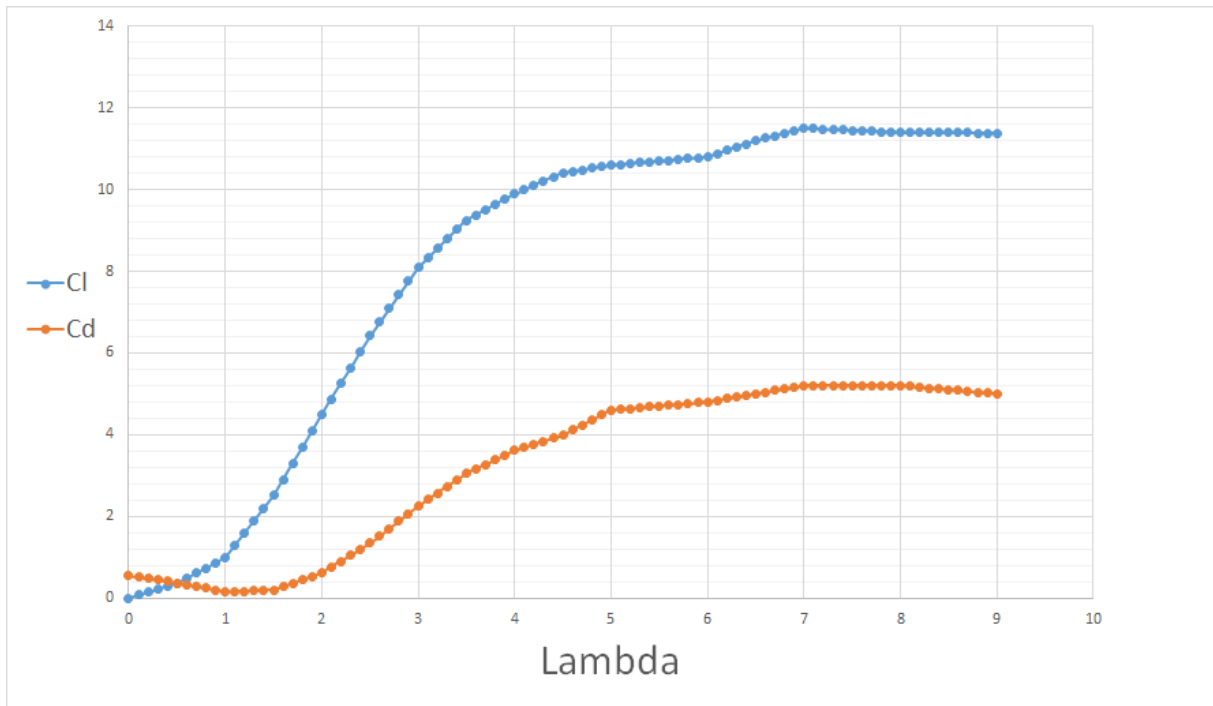


Figure 16: Lift and drag graph

The $Cl_{z,j}$ formula looks up the lift coefficient for each lambda value.

$$Cl_{z,j} := \text{vlookup}(\lambda_{r,z,j}, \lambda\text{Graph}, 1)_0 \quad Cl = \begin{bmatrix} 0.216 & 0.486 & 0.864 & 1.598 & 2.51 & 3.692 & 4.868 & 6.032 & 7.092 & 8.1 \\ 0.144 & 0.216 & 0.36 & 0.486 & 0.738 & 0.99 & 1.294 & 1.902 & 2.51 & 2.904 \\ 0.144 & 0.288 & 0.36 & 0.612 & 0.864 & 1.294 & 1.598 & 2.206 & 2.904 & 3.692 \\ 0.216 & 0.36 & 0.738 & 1.294 & 1.902 & 2.904 & 4.086 & 4.868 & 6.032 & 7.092 \dots \end{bmatrix}$$

The $Cd_{z,j}$ formula looks up the drag coefficient for each lambda value.

$$Cd_{z,j} := \text{vlookup}(\lambda_{r,z,j}, \lambda\text{Graph}, 2)_0 \quad Cd = \begin{bmatrix} 0.442 & 0.326 & 0.194 & 0.17 & 0.2 & 0.446 & 0.756 & 1.194 & 1.704 & 2.25 \\ 0.478 & 0.442 & 0.37 & 0.326 & 0.238 & 0.15 & 0.16 & 0.18 & 0.2 & 0.282 \\ 0.478 & 0.406 & 0.37 & 0.282 & 0.194 & 0.16 & 0.17 & 0.19 & 0.282 & 0.446 \\ 0.442 & 0.37 & 0.238 & 0.16 & 0.18 & 0.282 & 0.528 & 0.756 & 1.194 & 1.704 \dots \end{bmatrix}$$

4.7.4 Force calculation

When the apparent wind hits the ship, it creates a lift perpendicular to the apparent wind direction. At the same time, it will produce some drag parallel to the wind direction as a result of the wind pushing on the rotor. The direction of the lift depends on the direction of rotation. On a ship with a Flettner rotor you can easily change the direction of rotation in order to make the preferable lift. The sum between the lift force (F_L) and the drag force (F_D) will be the resulting force between the drag and lift (F_R).

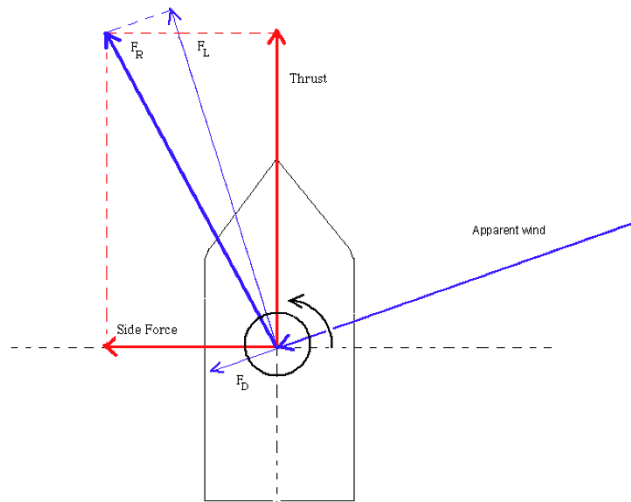


Figure 17: Flettner rotor force illustration

Source: Reproduced from Vahs, M (2018) Course material Green Shipping, Western Norway University of Applied Sciences, Haugesund. (Documents received from professor Michael Vahs)

The $F_{L,z,j}$ and $F_{D,z,j}$ is calculated in kN for each C_l and C_d value. In this formula, it is possible to add a second Flettner rotor to the calculations by multiplying the projected area (A_p) with 2.

$$F_{L,z,j} := C_{l,z,j} \cdot \left(\frac{\text{Rho} \cdot \text{AWS}_{z,0}^2 \cdot A_p \cdot 2}{2} \right) \quad F_L = \begin{bmatrix} 0.376 & 0.847 & 1.506 & 2.785 & 4.374 & 6.433 & 8.483 & 10.511 & 12.358 & 14.115 \\ 0.886 & 1.329 & 2.215 & 2.99 & 4.541 & 6.092 & 7.962 & 11.703 & 15.444 & 17.869 \\ 0.753 & 1.505 & 1.881 & 3.199 & 4.516 & 6.763 & 8.352 & 11.529 & 15.177 & 19.296 \\ 0.495 & 0.825 & 1.692 & 2.967 & 4.361 & 6.659 & 9.369 & 11.162 & 13.831 & 16.261 \dots \end{bmatrix} \text{ kN}$$

$$F_{D,z,j} := C_{d,z,j} \cdot \left(\frac{\text{Rho} \cdot \text{AWS}_{z,0}^2 \cdot A_p \cdot 2}{2} \right) \quad F_D = \begin{bmatrix} 0.77 & 0.568 & 0.338 & 0.296 & 0.349 & 0.777 & 1.317 & 2.081 & 2.969 & 3.921 \\ 2.941 & 2.72 & 2.277 & 2.006 & 1.464 & 0.923 & 0.985 & 1.108 & 1.231 & 1.735 \\ 2.498 & 2.122 & 1.934 & 1.474 & 1.014 & 0.836 & 0.888 & 0.993 & 1.474 & 2.331 \\ 1.013 & 0.848 & 0.546 & 0.367 & 0.413 & 0.647 & 1.211 & 1.733 & 2.738 & 3.907 \dots \end{bmatrix} \text{ kN}$$

This formula is calculating the resultant force ($Fr_{z,j}$), based on Fl and Fd.

$$Fr_{z,j} := \sqrt{\overrightarrow{Fl}_{z,j}^2 + \overrightarrow{Fd}_{z,j}^2} \quad Fr = \begin{bmatrix} 0.857 & 1.02 & 1.543 & 2.8 & 4.388 & 6.48 & 8.584 & 10.715 & 12.71 \\ 3.072 & 3.027 & 3.176 & 3.601 & 4.771 & 6.161 & 8.023 & 11.756 & 15.493 \\ 2.609 & 2.602 & 2.698 & 3.522 & 4.628 & 6.814 & 8.399 & 11.572 & 15.249 \\ 1.128 & 1.184 & 1.778 & 2.99 & 4.381 & 6.69 & 9.447 & 11.296 & 14.099 \dots \end{bmatrix} \text{ kN}$$

This formula defines where Apparent wind direction (AWD_r) would be in the fixed system.

$$AWD_r := \cos^{-1} \left(\frac{wd \cdot \beta}{Fr} \right) \quad AWD_r = \begin{bmatrix} 299.037 \\ 380.202 \\ 390.321 \\ 304.206 \end{bmatrix} \text{ deg}$$

This formula finds the lift force direction (FID_r) according to the fixed system.

$$FID_r := AWD_r + \overrightarrow{wd} \cdot 90 \text{ deg} - \left(\text{floor} \left(\frac{AWD_r + \overrightarrow{wd} \cdot 90 \text{ deg}}{360.01 \text{ deg}} \right) \cdot 360 \text{ deg} \right) \quad FID_r = \begin{bmatrix} 29.037 \\ 290.202 \\ 300.321 \\ 34.206 \end{bmatrix} \text{ deg}$$

This formula finds the resultant force direction (FrD_r) according to the fixed system.

$$FrD_{r,z,j} := \cos^{-1} \left(\frac{Fr_{z,j}}{Fr} \right) + FID_{r,z,0} \quad FrD_r = \begin{bmatrix} 92.992 & 62.89 & 41.692 & 35.109 & 33.592 & 35.925 & 37.864 & 40.233 \\ 216.968 & 226.247 & 244.418 & 256.349 & 272.328 & 281.587 & 283.154 & 284.796 \\ 227.086 & 245.672 & 254.536 & 275.582 & 287.666 & 293.272 & 294.249 & 295.398 \\ 98.161 & 79.99 & 52.08 & 41.254 & 39.612 & 39.752 & 41.569 & 43.033 \dots \end{bmatrix} \text{ deg}$$

This formula calculates the thrust (T) in heading direction for every different RPM scenarios.

$$T := Fr \cdot \cos(FrD_r) = \begin{bmatrix} -0.045 & 0.465 & 1.152 & 2.291 & 3.655 & 5.248 & 6.777 & 8.18 & 9.364 \\ -2.454 & -2.093 & -1.372 & -0.85 & 0.194 & 1.237 & 1.826 & 3.002 & 4.179 \\ -1.777 & -1.072 & -0.719 & 0.343 & 1.404 & 2.692 & 3.449 & 4.963 & 6.39 \\ -0.16 & 0.206 & 1.093 & 2.248 & 3.375 & 5.143 & 7.068 & 8.257 & 9.899 \dots \end{bmatrix} \text{ kN}$$

This is a Mathcad formula that looks up the optimal RPM ($optRPM_z$) for the maximum thrust value, and is demonstrated on the four examples below.

$$optRPM_z := \text{lookup} \left(MaxT_z, T_z^{\hat{z}}, T^{\hat{A}} \right)$$

Optimal RPM for wind direction case 1

$$optRPM_{0,0} = [230] \frac{1}{min}$$

Optimal RPM for wind direction case 2

$$optRPM_{1,0} = [130] \frac{1}{min}$$

Optimal RPM for wind direction case 3

$$optRPM_{2,0} = [170] \frac{1}{min}$$

Optimal RPM for wind direction case 4

$$optRPM_{3,0} = [170] \frac{1}{min}$$

The $MaxT_z$ formula looks up the highest value of thrust from the matrix produced in formula T .

$$MaxT_z := \max \left(T_z^{\hat{z}} \right) \quad MaxT_z = \begin{bmatrix} 13.122 \\ 5.979 \\ 11.221 \\ 14.597 \end{bmatrix} \text{ kN}$$

This is the final results that the calculator produces in this example.

4.7.5 Main calculation

All the calculations to produce the main result for this case study was done by the same approach as shown in the example above. The example only shows four different scenarios, but in reality this same procedure was done with every scenario of wind condition throughout the year.

Before these calculations could be done, the wind data from Eklima needed to be sorted. The wind speed and the wind direction from each day (attachment 4.1) was merged together into one common table. In order to do this the wind data was sorted into different

categories based on every 10° of wind direction. This resulted in a table showing the quantity of wind coming from each specific direction, as presented in the table in attachment 4.2.

For each calculation the appropriate wind direction was defined as tw and each wind speed for this specific direction was inserted in the matrix for ws . This was done for every directions between $30^\circ - 150^\circ$ and $210^\circ - 330^\circ$, the directions the Flettner rotor can produce forward thrust from. This calculated the amount of kN that was produced for each case, both when the ship is traveling north and south. The results from the calculator is presented in the table in attachment 5. In some cases with very low wind the answer in kN came out negative. In the table the negative values is written as 0, because the Flettner rotor can be shut down in these situations. Lastly all the kN produced throughout the year is summed up in the end of attachment 5. Based on these calculations, the Flettner rotor produced 2433,74 kN during one year in service. Further the total kN is used to calculate the following results presented in table 3 on the next page.

	A	B	C	D
1		Reference/Calculations	Value	Unit
2	Thrust in north course	From attachment 5	1213,74	kN
3	Thrust in south course	From attachment 5	1220,00	kN
4	Total thrust all year	C2+C3	2433,74	kN
5	Marine Diesel		0,88	kg/l
6	CO₂ factor for marine diesel	(Statistics Norway, 2016)	3,17	Kg CO ₂ /Kg fuel
7	Ship speed		5,10	m/s
8	Fuel consumption per day, without rotors	4.3.1 Fuel data for M/F Oppedal	2909,56	l
9	ETA_b engine efficiency		0,50	
10	Power efficiency	C4*C7	12412,06	kW
11	Engine power reduced yearly	C10/C9	24824,13	kW
12	Engine power reduced per day	C11/333 (amount of wind data days)	74,55	kW
13	Mass of fuel consumed in liter	4.3.1 Fuel data for M/F Oppedal	129,00	l/h
14	Mass of fuel consumed in g	C13*C5*1000	113520,00	g/h
15	Power develop	3.7.2 Fuel Data	800,00	kW
16	Sfoc	C14/C15	141,90	g/kW*h
17	Yearly hours	Attachment 6	5373,00	h
18	Hours per day	C17/365	14,72	h
19	Fuel saved per day in Kg	C18*C12*C16/1000	155,72	kg
20	Fuel saved per day in liter	C19/C5	176,95	l
21	Fuel saved in percentage	(C20/C8)*100	6,08	%
22	Fuel price	Bunker Oil AS: 4,73kr +1,35kr	6,08	kr
23	Money saved per day	C20*C22	1075,86	kr
24	Money saved per year	C23*365	392690,06	kr
25	Flettner rotor installation cost	4.4.1 Provided assessment of installation cost	6764660,00	kr
26	down time payment	C25/C24	17,23	years
27	CO₂ saved per day in kg	C19*C6	493,62	kg
28	CO₂ saved per day in tonnes	C27/1000	0,49	tonnes
29	CO₂ saved per year	C28*365	180,17	tonnes

Table 3: Final calculations

5. Results

The following tables shows the results from this case study regarding visibility requirements by SOLAS, stability requirements by IMO and NMA and the calculated effect from the Flettner rotor:

Visibility and stability requirements:

Visibility requirements accordance to SOLAS	OK
Stability requirements according to IMO's code on intact Stability	OK (Small adjustments needs to be done with the maximum GZ in fully loaded condition)
Stability requirements according to NMA	OK

Table 4: Visibility and stability results

Result of the Flettner Rotor instalment:

Average fuel saved per day in kg	155,7 kg
Average fuel saved in percentage	6,1 %
Average CO ₂ saved per day	493,6 kg
Average CO ₂ saved per year	180 tonnes
Average fuel cost saved per day	1 079 NOK
Average fuel cost saved per year	392 690 NOK
Down time payment	≈ 17 years

Table 5: Result of Flettner rotor instalment

6. Discussion

6.1 Answering the thesis statement

To answer the thesis statement, “*Can Flettner rotor be a feasible technical solution for ferries in Norway as a means to reach a lower environmental impact?*”, the term feasible is key to understand. As previously explained in chapter 1.1 the term used in this paper is mainly based on two things. First of all, it is the possibility to implement this technical solution on the M/F “Oppedal” as in accordance with regulations by SOLAS, IMO and NMA. Secondly it is the down time payment, which is the price of the investment in relation to the yearly savings. Ship owners investing in such new technology will most likely prefer a period of time until the investment is earned back, should it even be considered.

The technical possibility was fulfilled as both the stability- and visibility calculations proved that the instillation of the rotors would be in accordance with regulations. It should however be noted that some small adjustments may need to be made, if the maximum GZ in fully loaded condition shall be in compliance with regulations. In addition to this the calculation of the blindzone created by the rotor revealed a small margin of only $0,1^\circ$ compared to the stated regulations. It may be advised to locate the rotors even further from the bridge to achieve a higher margin, but according to calculations in our case no regulations would be breached.

The down time payment reached from calculations was higher than initially expected. The cost of installing the two rotors would amount to a total of 700 000 euros, equal to 6 764 660 Norwegian kroners by today’s (25.04.2019) currency. The money saved per year in marine diesel oil was calculated to be 392 690 Norwegian kroners. By dividing the two, an expected down time payment of approximately 17 years was calculated. This means that 17 years would pass before the investment of almost 7 millions Norwegian kroners is earned back, and the ship owner could collect from the economical advantages from the instillation. In the one hand it is not likely that anyone would invest in something that takes 17 years to earn back, but on the other hand the Flettner rotors will save 6,1 % of the total fuel consumption. This will have a positive impact in order to lower the ship’s environmental impact.

6.2 Hypothesis

The hypothesis in this case study was that the result from the calculations could be applied for other ferries operating in similar conditions with comparable parameters. This is one of the reasons why a case study was chosen as the appropriate method in the first place. The result would not only be confined to this route, but general conclusions could be drawn onto other cases. If Norway is going to be in line with international climate conventions such as The Paris Agreement, the technical solution needed to apply for more than one case. This is why this specific route as a part of E39 was chosen, with the assumption that the ferry routes along E39 will have somewhat similar conditions.

The government did not set the completion of a ferry free E39 in their NNT of 2017 to any specific year and the price of the project is reaching proportions that might stop the whole process altogether. Transitional solutions such as the Flettner rotor, could lower the CO₂ emissions in accordance with international climate conventions. The installation of two Flettner rotors on M/F “Oppedal” was calculated to reduce the fuel consumption by 6,1 %, equal to a 180 tonnes reduction of CO₂ yearly. This may not seem that much, but by comparing it with a car that produces an average of 120,5 g CO₂ per km (Jato, 2019), the car could drive 37 times the distance around equator with an equivalent amount of emissions. If this was a solution implemented on all Norwegian ferries, given that they experienced similar results as calculated in this case, it might be a part solution to reaching the climate goal set forth in The Paris Agreement. Still it would probably have to be subsidised by the government in some sort of way, because of the duration of the down time payment.

6.3 Comparing the result with other cases

Norway is a country with a long coastline consisting of many fjords. Naturally there are ferries crossing most of these fjords, like M/F “Oppedal”. Supposing most of these ferries are more or less of the same size as M/F “Oppedal” and with similar wind conditions following the fjord, they may produce the same results as this case study. With this in mind, the possibility to install Flettner rotors of the same dimensions, is most likely there. With the Mathcad calculator made for this study, it is possible to redefine the variables to match other

cases and estimate saved fuel cost for each specific ferry. However for this case, there are still some factors and parameters that could have affected the final result of this study.

6.4 Actual effect VS Theoretical effect

According to professor Michael Vahs, the actual effect of the Flettner rotor during sea trails has proven to be between 10-40 % higher than the predicted effect from the calculations. As this study is based on his calculation method, it might be expected to experience similar increase of effect if the Flettner rotors would be tested on M/F “Oppedal”.

6.5 Mean wind

The calculations in this thesis are based on average mean wind throughout the day, but wind often differ in speed and direction during the day. Wind gusts can sometimes come in short periods with a great increase in speed and the effect of the Flettner rotors will in such cases increase significantly.

6.6 Takle´s location compared to the route

The location of Takle weather station is somewhat off, compared to the route. As figure 18 illustrates, the windrose has been placed on top of the weather station. The fjord is shaped around the headland south west of Lavik. It is possible that the wind will somewhat change direction as it flows around this headland. If this is the case, there would probably be less wind directly from north

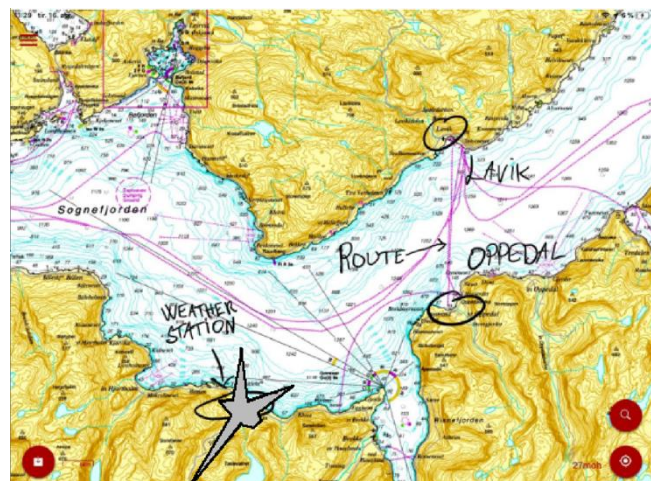


Figure 18: Lavik-Oppedal route location with wind rose

in the location of the route, and it would be more wind coming from south-west. This change

in wind direction could have a significant impact on the effect of the Flettner rotor, as the wind from the north will not provide the ship with any thrust in heading direction. In addition to this it is possible that the weather station is located in a more leeward position from the wind compared to the route, and that the wind present in the route location will be stronger.

6.7 Increase in CO2 tax

According to Bunker Oil AS, where the fuel prices were gathered from, the CO2 taxes are increasing every year. The recent focus given to the environment and climate could result in a significant rise in CO₂ taxes. This would affect our result as more amount of saved fuel cost would result in a faster down time payment.

-

7. Conclusion

All things considered makes it very difficult to confirm whether or not the question, *Can Flettner rotor be a feasible technical solution for ferries in Norway in order to reach a lower environmental impact?*, really is answered. This thesis has proven beyond any doubt, that the requirements to stability and visibility after instillation of the Flettner rotors are met in the case of M/F “Oppedal”. Yet, equally important is the other part of the feasibility term. It is the result of this case study that a calculated saved fuel cost of 6,1 % would still amount to 17 years, before the rotors are profitable. Such an investments usually needs to be profitable within a certain amount of time, if it shall be installed. However, all the different parameters affecting this case could shift the result in either direction and rising fuel taxes might reduce the expected down time payment.

The 180 tonnes reduction of CO₂ emissions yearly would be one small step in the right direction, if Norway were to uphold the commitments in The Paris Agreement. Assuming the calculation of other similar cases along E39 would yield the same result as in this case, then it could be a big step. The Mathcad calculator developed in this study could easily be used again for other cases with different parameters. In light of all these findings the paper ends with former Norwegian prime minister Kåre Willoch (Arendalsuka, 2018, 11:45)

*But I want to add,
take this opportunity to make an admonition to these so-called climate sceptics.
Because the world probably still has a lot of people
who refuse to believe that humans are affecting the climate.
And want to postpone actions until we can see if it works,
if it is actually humans affecting the climate. To them I want to say
You cannot answer firmly and with 100% safety that yes humans are ruining this,
but you most definitely cannot say no either. The question is:
Is there a risk that our emission of gasses is affecting the climate? And this can no one deny,
there is a very high risk and if there is a high risk then we must take measures,
even though we are not 100% sure.*

Sources

Arendalsuka. (2018, 14. aug). *Den store samtalen* [Videoklipp]. Retrieved from:

<https://www.youtube.com/watch?v=HqBKfk4dkVk&t=691s>

Climate Action Tracker. (n.d.a). Retrieved 24th april 2019 from:

<https://climateactiontracker.org/>

Climate Action Tracker. (n.d.b) *Norway*. Retrieved 24th april 2019 from:

<https://climateactiontracker.org/countries/norway/>

Curley, R. (2011). *The Complete History of Ships and Boats: From Sails and Oars to Nuclear-Powered Vessels*, Britannica Educational Publishing.

Da-Qing, L., Leer-Andersen, M., & Allenström, B. (2012). *Performance and vortex formation of Flettner rotors at high Reynolds numbers*. Proceedings of 29th Symposium on Naval Hydrodynamics.

Dahlum, S. & Wæhle, E. *Case-studie*. Store norske leksikon. Retrieved 10. april 2019 from

<https://snl.no/case-studie>

Falkner, R. (2016). The Paris Agreement and the new logic of international climate politics. *International Affairs*, 92(5), 1107-1125. Retrieved from:

<https://academic.oup.com/ia/article/92/5/1107/2688148>

Forskrift om bygging av skip (2014). Forskrift om bygging av skip (FOR-2014-07-01-1072).

Retrieved from <https://lovdata.no/dokument/SF/forskrift/2014-07-01-1072/>

Freese, Niels. (2017). *CO₂ Emissions from International Maritime Shipping*. UNEP DTU PARTNERSHIP. Retrieved from: <http://www.unepdtu.org/>-

[/media/Sites/Uneprioe/Working-Papers/2017/Working-Paper-4_Emissions-from-Shipping.ashx?la=da&hash=F8FC98CB8712757219146CEBD6B651EA5E0051D4](http://www.unepdtu.org/-/media/Sites/Uneprioe/Working-Papers/2017/Working-Paper-4_Emissions-from-Shipping.ashx?la=da&hash=F8FC98CB8712757219146CEBD6B651EA5E0051D4)

Gilmore, C. (1984). "Spin sail harnesses mysterious Magnus effect for ship propulsion."

Popular Science: 70-72.

Hope, Vidar. (2019). Ferjefri E39 er vinnar av “sløseri-pris”. *Sunnhordland*. Retrieved from:
<http://www.sunnhordland.no/nyhende/ferjefri-e39-er-vinnar-av-sloseri-pris-1.2597909>

Intergovernmental Panel on Climate Change (2019). Special Report: Global Warming of 1.5°C. *Summary for policymakers*. Retrieved from:
https://www.ipcc.ch/site/assets/uploads/sites/2/2018/07/SR15_SPM_version_stand_alone_LR.pdf

IS-Code (2008). Adoption of the international code on intact stability, 2008. (RESOLUTION MSC.267(85)(2008, 4. December)). Retrieved from:
[http://www.imo.org/en/KnowledgeCentre/IndexofIMOResolutions/Maritime-Safety-Committee-\(MSC\)/Documents/MSC.267\(85\).pdf](http://www.imo.org/en/KnowledgeCentre/IndexofIMOResolutions/Maritime-Safety-Committee-(MSC)/Documents/MSC.267(85).pdf)

IMO (2014). *SOLAS Consolidated edition 2014: Consolidated text of the International Convention for the Safety of Life at Sea, 1974, and its Protocol of 1988: Articles, annexes and certificates: Incorporating all amendments in effect from 1 July 2014*. London: IMO

Jacobsen, D. I. (2015). *Hvordan gjennomføre undersøkelser* (3rd edition). Cappelen Damm AS

Jato (2019). *CO2 Emissions rise to highest average since 2014, as the shift from diesel to gasoline continues*. Retrieved from: <https://www.jato.com/wp-content/uploads/2019/03/CO2-Europe-2018-Release-Final.pdf>

Kjerstad, N. (2013). *Fremføring av skip med navigasjonskontroll for maritime studier*. (3rd edition). Akademika Forlag

Multi Maritime A/S. (2008). *Trim- & Stabilitetsbok M/F “Tidesund”, IMO 9419216*. (60152112). (document received from Norled). Førde: Multi Maritime A/S

Norges Bank (2019, 25. April). *Valutakurser*. Retrieved from: <https://www.norges-bank.no/tema/Statistikk/valutakurser/?id=EUR>

- Norled (2018) *E39 Lavik - Oppedal*. Retrieved 22.04.2019 from
https://www.norled.no/contentassets/a4aa7bd2b2304c6d8aaf5df4c97a4d94/lavik-oppedal_rute1046_k3-2019.pdf
- Norsepower (n.d.a) *References*. Retrieved 03.04.2019 from
<https://www.norsepower.com/references>
- Norsepower (n.d.b). *Technology*. Retrieved 11.04.2019 from
<https://www.norsepower.com/technology>
- NRK Sogn og Fjordane. (2002, 17. oktober). *E 39 mellom Sogn og Bergen*. Retrieved 11.04.2019 from
https://www.nrk.no/nyheter/distrikt/nrk_sogn_og_fjordane/fylkesleksikon/2220359.html
- Nuttall, P. & J. Kaitu'u (2016). "The Magnus Effect and the Flettner Rotor: potential application for future Oceanic Shipping." *J. Pac. Stud.*
- Reid, F. (1997). *The Magnus Effect*, Parabola.
- Rohden, R. (2012). *Magnus rotor*. United States Patent.
- Samferdselsdepartementet. (2013). *Nasjonal Transportplan* (Meld. St. 26 (2012-2013)).
Retrieved from: <https://www.regjeringen.no/no/dokumenter/meld-st-26-20122013/id722102/>
- Samferdselsdepartementet. (2017). *Nasjonal Transportplan* (Meld. St. 33 (2016-2017)).
Retrieved from: <https://www.regjeringen.no/no/dokumenter/meld.-st.-33-20162017/id2546287/>
- Schmidt, A. (2013a, September). *E-ship 1 - A wind-hybrid commercial cargo ship*. Presented at International conference on ship efficiency - 2013, Hamburg. Retrieved from <https://www.stg-online.org/onTEAM/shipefficiency/programm/06-Andreas-Schmidt.pdf>

- Schmidt, A. (2013b, September). *E-ship 1 - A wind-hybrid commercial cargo ship*. Presented at International conference on ship efficiency - 2013, Hamburg. Retrieved from https://www.stg-online.org/onTEAM/shipefficiency/programm/06-STG_Ship_Efficiency_2013_100913_Paper.pdf
- Seifert, J. (2012). *A review of the Magnus effect in aeronautics*. *Progress in Aerospace Sciences* **55**: 17-45.
- Seybold, G. (1925). "A sailing ship without sails: new wonder of the seas." *Popular Science Monthly*, February.
- Skipsrevyen (2008). M/F "Tidesund". *Skipsrevyen*. Retrieved from <https://www.skipsrevyen.no/batomtaler/m-f-tidesund/>
- Statens Vegvesen. (2016, 22 June). *Ferjerfri E39 - klimaeffekter*. Retrieved from: <https://www.vegvesen.no/vegprosjekter/ferjerfriE39/rapportar>
- Statens Vegvesen. (n.d.). *Ferjerfri E39*. Retrieved from: <https://www.vegvesen.no/vegprosjekter/ferjerfriE39?fbclid=IwAR3i3jYSt1-OQsf7MjwnZ3Kq7gQU3w0sIVKwJCuMhG69SBgeTeUzHB3FqGw>
- Statistics Norway (2016). *The Norwegian Emission Inventory 2016*. Retrieved from: https://www.ssb.no/en/natur-og-miljo/artikler-og-publikasjoner/_attachment/279491?_ts=1576a6ddf40
- Svendsen, S. W. (2006). *Stratification and circulation in Sognefjorden*. The University of Bergen.
- United Nations. (2015). *The Paris Agreement*. Retrieved from: https://unfccc.int/files/essential_background/convention/application/pdf/english_paris_agreement.pdf
- Vahs, M. (2018). *Course Material Green Shipping*. Western Norway University of Applied Sciences, Haugesund. (documents received from Professor Michael Vahs)

Vahs, M., Stybny, J., Peetz, T., Götting, M., Müller, M., & Strasser, S. (2019). Flettner Rotor Senkt Brennstoffkosten. *Schiff & Hafen*. 71(02), 12-20.

Viking Line (2018). *Annual report 2018*. Retrieved from https://www.vikingline.com/globalassets/documents/market_specific/corporate/investors/annual-reports/annual-report-2018.pdf

World Maritime News. (2018, 14. December). *Flettner Rotor-Fitted Ultramax Wins Ship of the Year Award*. Retrieved 11.09.2019 from <https://worldmaritimeneeds.com/archives/266727/flettner-rotor-fitted-ultramax-wins-ship-of-the-year-award/>

World Wide Fund for Nature. (n.d.). *Coral Reefs*. Retrieved 23.04.2019 from: https://wwf.panda.org/our_work/oceans/coasts/coral_reefs/

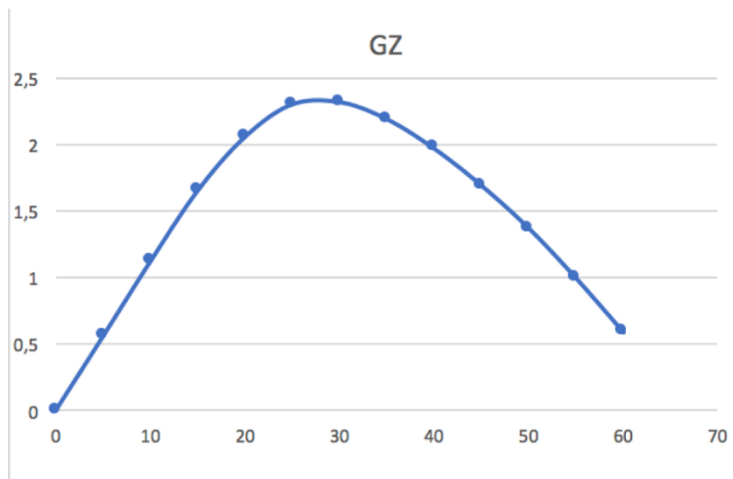
Wåge, J. (2019, 29 March). Klimastreik: Eit nytt ungdoms-opprør er i gang. *Dagbladet*. Retrieved from: <https://www.dagbladet.no/kultur/eit-nytt-ungdoms-oppror-er-i-gang/70911685>

Attachments

Attachement 1. Stability calculations.

LIGHT SHIP			
	WEIGHT (TONNES)	VCG/KG (METERS)	MOMENT (TONNES*METERS)
SHIP WITHOUT ROTORS	1705,1	5,487	9355,8837
ROTOR 1	29	13,5	391,5
ROTOR 2	29	13,5	391,5
SUM	1763,1		10138,8837
TOTAL VCG/KG =	TOTAL MOMENT/TOTAL WEIGHT =		5,750600476

KG	Angle	KG*sin(angle)	KY	GZ
5,750600476	0	0	0	0
5,750600476	5	0,501197856	1,059	0,557802144
5,750600476	10	0,998581293	2,118	1,119418707
5,750600476	15	1,488364924	3,14	1,651635076
5,750600476	20	1,966821199	4,024	2,057178801
5,750600476	25	2,430308777	4,733	2,302691223
5,750600476	30	2,875300238	5,196	2,320699762
5,750600476	35	3,298408928	5,491	2,192591072
5,750600476	40	3,696414734	5,668	1,971585266
5,750600476	45	4,066288592	5,76	1,693711408
5,750600476	50	4,405215539	5,778	1,372784461
5,750600476	55	4,710616136	5,708	0,997383864
5,750600476	60	4,980166099	5,572	0,591833901

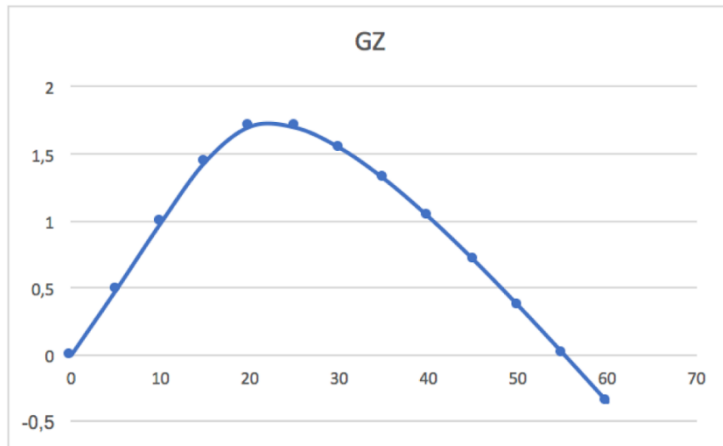


Simson's factor	GZ	GZ*Simson's factor
1	0	0
4	0,557802144	2,231208577
2	1,119418707	2,238837414
4	1,651635076	6,606540304
1	2,057178801	2,057178801
SUM=		13,1337651
Area under the GZ-curve 0-20 degrees		
$(5/3)*(PI/180)*(Sum\ of\ simson's\ factor)$		
		0,38204574 > 0,055

Simson's factor	GZ	GZ*Simson's factor	Simsons factor	GZ	GZ*Simson's factor
1	0	0	1	0	0
4	0,557802144	2,231208577	4	1,119418707	4,477674827
2	1,119418707	2,238837414	2	2,057178801	4,114357602
4	1,651635076	6,606540304	4	2,320699762	9,282799048
2	2,057178801	4,114357602	1	1,971585266	1,971585266
4	2,302691223	9,210764891	SUM=		19,84641674
1	2,320699762	2,320699762			
SUM=		26,72240855			
Area under the GZ-curve 0-30 degrees			Area under the GZ-curve 0-40 degrees		
$(5/3)*(PI/180)*(Sum\ of\ simson's\ factor)$			$(10/3)*(PI/180)*(sum\ of\ simspson's\ factor)$		
		0,777323355 > 0,055			1,154617723 > 0,09
Area under the GZ-curve 30-40 degrees			Area(0-40degrees)-Area(0-30degrees)		
					0,37729437 > 0,03

FULLY LOADED SHIP			
	WEIGHT (TONNES)	VCG/KG (METERS)	MOMENT (TONNES*METERS)
SHIP WITHOUT ROTORS	2625,6	5,889	15462,1584
ROTOR 1	29	13,5	391,5
ROTOR 2	29	13,5	391,5
SUM	2683,6		16245,1584
TOTAL VCG/KG =		TOTAL MOMENT/TOTAL WEIGHT =	6,053494709

KG	Angle	KG*sin(angle)	KY	GZ
6,053494709	0	0	0	0
6,053494709	5	0,527596828	1,014	0,486403172
6,053494709	10	1,051178325	2,039	0,987821675
6,053494709	15	1,56675972	3,014	1,44724028
6,053494709	20	2,070417128	3,78	1,709582872
6,053494709	25	2,558317411	4,261	1,702682589
6,053494709	30	3,026747355	4,578	1,551252646
6,053494709	35	3,472141923	4,79	1,317858077
6,053494709	40	3,891111394	4,923	1,031888606
6,053494709	45	4,280467159	4,993	0,712532841
6,053494709	50	4,637245983	5,007	0,369754017
6,053494709	55	4,958732566	4,971	0,012267434
6,053494709	60	5,2424802	4,889	-0,3534802



Simpson's factor	GZ	GZ*Simpson's factor
1	0	0
4	0,486403172	1,94561269
2	0,987821675	1,975643351
4	1,44724028	5,78896112
1	1,709582872	1,709582872
SUM=		11,41980003
Area under the GZ-curve 0-20 degrees		
(5/3)*(PI/180)*(Sum of simson's factor)		0,332188517 >0,055

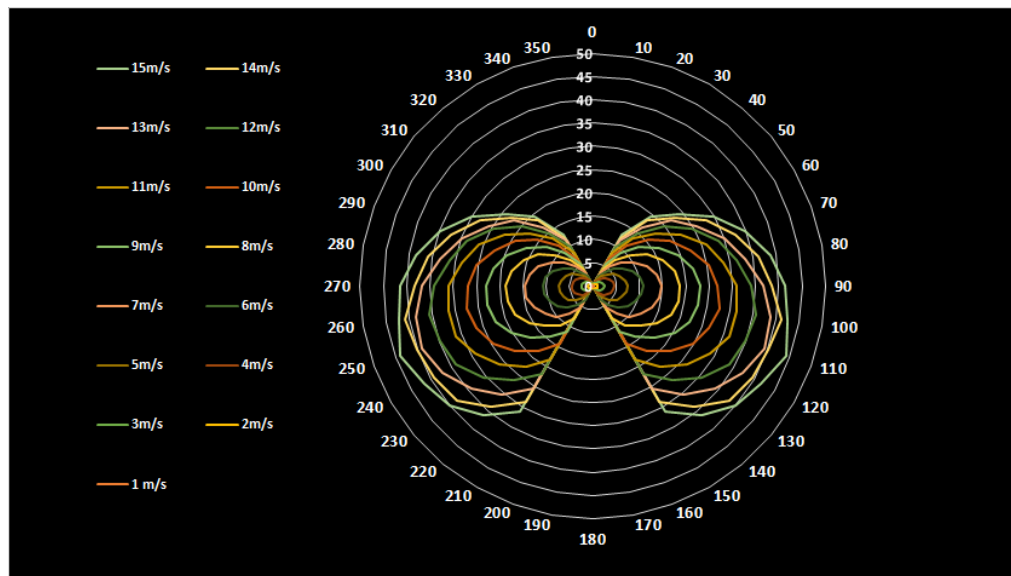
Simpson's factor	GZ	GZ*Simpson's factor	Simpson's factor	GZ	GZ*Simpson's factor
1	0	0	1	0	0
4	0,486403172	1,94561269	4	0,987821675	3,951286701
2	0,987821675	1,975643351	2	1,709582872	3,419165744
4	1,44724028	5,78896112	4	1,551252646	6,205010582
2	1,709582872	3,419165744	1	1,031888606	1,031888606
4	1,702682589	6,810730355	SUM=		14,60735163
1	1,551252646	1,551252646	SUM=		21,4913659
Area under the GZ-curve 0-30 degrees			Area under the GZ-curve 0-40 degrees		
(5/3)*(PI/180)*(Sum of simson's factor)		0,625158493 >0,055	(10/3)*(PI/180)*(sum of simspson's factor)		0,84982127 >0,09
Area under the GZ-curve 30-40 degrees			Area(0-40degrees)-Area(0-30degrees)		0,22466278 >0,03

Attachment 2. Polar plot.

The thrust effect of one Flettner in different wind speed and wind directions.

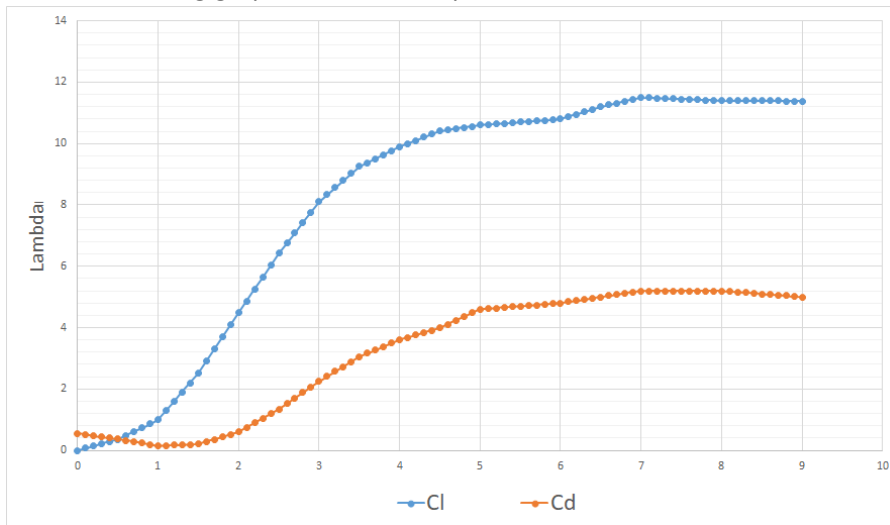
	0	10	20	30	40	50	60	70	80	90	100	110	120	130	140	150	160	170	180
1 m/s	0,00	0,00	0,00	0,00	0,04	0,12	0,16	0,20	0,25	0,25	0,24	0,22	0,18	0,13	0,09	0,00	0,00	0,00	0,00
2m/s	0,00	0,00	0,00	0,22	0,41	0,62	0,84	0,95	1,04	1,07	1,05	0,94	0,82	0,63	0,44	0,26	0,00	0,00	0,00
3m/s	0,00	0,00	0,00	0,56	0,96	1,43	1,82	2,15	2,39	2,48	2,42	2,22	1,90	1,48	1,04	0,61	0,00	0,00	0,00
4m/s	0,00	0,00	0,00	1,08	1,84	2,55	3,27	3,88	4,34	4,55	4,55	4,20	3,62	2,90	2,06	1,24	0,00	0,00	0,00
5m/s	0,00	0,00	0,00	1,68	2,79	3,98	5,14	6,18	6,97	7,41	7,29	6,69	6,00	4,80	3,43	2,12	0,00	0,00	0,00
6m/s	0,00	0,00	0,00	2,40	4,01	5,79	7,51	9,05	10,24	10,83	10,61	9,73	8,72	7,23	5,32	3,44	0,00	0,00	0,00
7m/s	0,00	0,00	0,00	3,41	5,56	7,89	10,31	12,45	13,90	14,66	14,57	13,45	11,86	10,22	7,86	5,38	0,00	0,00	0,00
8m/s	0,00	0,00	0,00	4,41	7,29	10,43	13,49	15,94	17,79	18,65	18,63	17,81	15,81	13,34	11,05	8,01	0,00	0,00	0,00
9m/s	0,00	0,00	0,00	5,51	9,21	12,98	16,51	19,60	21,75	23,00	23,02	22,23	20,27	17,41	14,14	11,26	0,00	0,00	0,00
10m/s	0,00	0,00	0,00	6,73	11,34	15,55	19,32	22,38	25,35	26,73	27,63	26,62	24,78	21,83	18,24	14,30	0,00	0,00	0,00
11m/s	0,00	0,00	0,00	8,07	13,28	17,65	21,98	26,03	28,50	30,91	31,35	31,33	29,18	26,30	22,47	18,28	0,00	0,00	0,00
12m/s	0,00	0,00	0,00	9,58	14,75	19,92	24,69	28,71	31,30	34,05	35,62	34,93	33,87	30,59	26,45	21,96	0,00	0,00	0,00
13m/s	0,00	0,00	0,00	11,14	16,57	22,10	25,86	30,01	33,19	36,72	38,65	39,16	37,25	34,15	30,28	25,46	0,00	0,00	0,00
14m/s	0,00	0,00	0,00	11,91	18,33	22,95	28,06	32,55	36,08	38,34	41,09	40,09	39,52	38,16	33,96	28,62	0,00	0,00	0,00
15m/s	0,00	0,00	0,00	12,62	19,31	24,04	30,02	34,82	38,68	41,27	42,37	44,10	41,74	40,01	36,36	31,27	0,00	0,00	0,00

	180	190	200	210	220	230	240	250	260	270	280	290	300	310	320	330	340	350
1 m/s	0,00	0,00	0,00	0,00	0,09	0,13	0,18	0,22	0,24	0,25	0,25	0,20	0,16	0,12	0,04	0,00	0,00	0,00
2m/s	0,00	0,00	0,00	0,26	0,44	0,63	0,82	0,94	1,05	1,07	1,04	0,95	0,84	0,62	0,41	0,22	0,00	0,00
3m/s	0,00	0,00	0,00	0,61	1,04	1,48	1,90	2,22	2,42	2,48	2,39	2,15	1,82	1,43	0,96	0,56	0,00	0,00
4m/s	0,00	0,00	0,00	1,24	2,06	2,90	3,62	4,20	4,55	4,55	4,34	3,88	3,27	2,55	1,84	1,08	0,00	0,00
5m/s	0,00	0,00	0,00	2,12	3,43	4,80	6,00	6,99	7,29	7,41	6,97	6,18	5,14	3,98	2,79	1,68	0,00	0,00
6m/s	0,00	0,00	0,00	3,44	5,32	7,23	8,72	9,73	10,61	10,83	10,24	9,05	7,51	5,79	4,01	2,40	0,00	0,00
7m/s	0,00	0,00	0,00	5,38	7,86	10,22	11,86	13,45	14,57	14,66	13,90	12,45	10,31	7,89	5,56	3,41	0,00	0,00
8m/s	0,00	0,00	0,00	8,01	11,05	13,34	15,81	17,81	18,63	18,65	17,79	15,94	13,49	10,43	7,29	4,41	0,00	0,00
9m/s	0,00	0,00	0,00	11,26	14,14	17,41	20,27	22,23	23,02	23,00	21,75	19,60	16,51	12,98	9,21	5,51	0,00	0,00
10m/s	0,00	0,00	0,00	14,30	18,24	21,83	24,78	26,62	27,63	26,73	25,35	22,38	19,32	15,55	11,34	6,73	0,00	0,00
11m/s	0,00	0,00	0,00	18,28	22,47	26,30	29,18	31,33	31,35	30,91	28,50	26,03	21,98	17,65	13,28	8,07	0,00	0,00
12m/s	0,00	0,00	0,00	21,96	26,45	30,59	33,87	34,93	35,62	34,05	31,30	28,71	24,69	19,92	14,75	9,58	0,00	0,00
13m/s	0,00	0,00	0,00	25,46	30,28	34,15	37,25	39,16	38,65	36,72	33,19	30,01	25,86	22,10	16,57	11,14	0,00	0,00
14m/s	0,00	0,00	0,00	28,62	33,96	38,16	39,52	40,09	41,09	38,34	36,08	32,55	28,06	22,95	18,33	11,91	0,00	0,00
15m/s	0,00	0,00	0,00	31,27	36,36	40,01	41,74	44,10	42,37	41,27	38,68	34,82	30,02	24,04	19,31	12,62	0,00	0,00



Attachment 3. Lift and drag graph

The Lift and drag graph with the interpolations



lambda	Cl	Cd	lambda	Cl	Cd	lambda	Cl	Cd
0	0	0,55	3	8,1	2,25	6	10,8	4,8
0,1	0,072	0,514	3,1	8,33	2,41	6,1	10,88	4,84
0,2	0,144	0,478	3,2	8,56	2,57	6,2	10,96	4,88
0,3	0,216	0,442	3,3	8,79	2,73	6,3	11,04	4,92
0,4	0,288	0,406	3,4	9,02	2,89	6,4	11,12	4,96
0,5	0,36	0,37	3,5	9,25	3,05	6,5	11,2	5
0,6	0,486	0,326	3,6	9,38	3,162	6,6	11,26	5,04
0,7	0,612	0,282	3,7	9,51	3,274	6,7	11,32	5,08
0,8	0,738	0,238	3,8	9,64	3,386	6,8	11,38	5,12
0,9	0,864	0,194	3,9	9,77	3,498	6,9	11,44	5,16
1	0,99	0,15	4	9,9	3,61	7	11,5	5,2
1,1	1,294	0,16	4,1	10,002	3,686	7,1	11,49	5,2
1,2	1,598	0,17	4,2	10,104	3,762	7,2	11,48	5,2
1,3	1,902	0,18	4,3	10,206	3,838	7,3	11,47	5,2
1,4	2,206	0,19	4,4	10,308	3,914	7,4	11,46	5,2
1,5	2,51	0,2	4,5	10,41	3,99	7,5	11,45	5,2
1,6	2,904	0,282	4,6	10,448	4,112	7,6	11,44	5,2
1,7	3,298	0,364	4,7	10,486	4,234	7,7	11,43	5,2
1,8	3,692	0,446	4,8	10,524	4,356	7,8	11,42	5,2
1,9	4,086	0,528	4,9	10,562	4,478	7,9	11,41	5,2
2	4,48	0,61	5	10,6	4,6	8	11,4	5,2
2,1	4,868	0,756	5,1	10,62	4,62	8,1	11,4	5,18
2,2	5,256	0,902	5,2	10,64	4,64	8,2	11,4	5,16
2,3	5,644	1,048	5,3	10,66	4,66	8,3	11,4	5,14
2,4	6,032	1,194	5,4	10,68	4,68	8,4	11,4	5,12
2,5	6,42	1,34	5,5	10,7	4,7	8,5	11,4	5,1
2,6	6,756	1,522	5,6	10,72	4,72	8,6	11,396	5,08
2,7	7,092	1,704	5,7	10,74	4,74	8,7	11,392	5,06
2,8	7,428	1,886	5,8	10,76	4,76	8,8	11,388	5,04
2,9	7,764	2,068	5,9	10,78	4,78	8,9	11,384	5,02
3	8,1	2,25	6	10,8	4,8	9	11,38	5

lambda	Cl	Cd	lambda	Cl	Cd
9,1	11,38	5	12,1	11,38	5
9,2	11,38	5	12,2	11,38	5
9,3	11,38	5	12,3	11,38	5
9,4	11,38	5	12,4	11,38	5
9,5	11,38	5	12,5	11,38	5
9,6	11,38	5	12,6	11,38	5
9,7	11,38	5	12,7	11,38	5
9,8	11,38	5	12,8	11,38	5
9,9	11,38	5	12,9	11,38	5
10	11,38	5	13	11,38	5
10,1	11,38	5	13,1	11,38	5
10,2	11,38	5	13,2	11,38	5
10,3	11,38	5	13,3	11,38	5
10,4	11,38	5	13,4	11,38	5
10,5	11,38	5	13,5	11,38	5
10,6	11,38	5	13,6	11,38	5
10,7	11,38	5	13,7	11,38	5
10,8	11,38	5	13,8	11,38	5
10,9	11,38	5	13,9	11,38	5
11	11,38	5	14	11,38	5
11,1	11,38	5	14,1	11,38	5
11,2	11,38	5	14,2	11,38	5
11,3	11,38	5	14,3	11,38	5
11,4	11,38	5	14,4	11,38	5
11,5	11,38	5	14,5	11,38	5
11,6	11,38	5	14,6	11,38	5
11,7	11,38	5	14,7	11,38	5
11,8	11,38	5	14,8	11,38	5
11,9	11,38	5	14,9	11,38	5
12	11,38	5	15	11,38	5

lambda	Cl	Cd
15,1	11,38	5
15,2	11,38	5
15,3	11,38	5
15,4	11,38	5
15,5	11,38	5

Attachment 4. Wind data.

Attachment 4.1

Wind direction

Date	Jan	Feb	Mar	Apr	May	Jun	Jul	Aug	Sep	Oct	Nov	Dec
1	220	0	320	100	230	300	0	310	70	220	220	300
2	220	340	270	80	230	290	330		0	150	80	90
3	270	150	220	80	160	320	220		0	0	90	220
4	220	70		60	0	300	150		160	0	220	260
5	90	150	0	10	0	340	220		160	220	0	340
6	0	220	0	160	90	160	190	0	0	220	220	340
7	240	220	220	340	90	220	230	320	0	0	160	230
8	70	220	110	110	110	300	220	260	210	220	90	60
9	70	220	70	70	70	300	220	0	0		210	80
10	220	220	0	70	0	160	320	0	0		230	220
11	220	220	70	70	0	340	20	290	340		130	120
12	220	220	320	70	230	320	300	220	340		220	240
13	200	150	60	340	220	130	270	340	320		240	220
14	70	140	80	160	30	220	240	340	0		160	230
15	80	80	70		90	70	220	80	160		230	220
16	70	160	70		50	300	0	90	0		240	0
17	220	70	120			50	220	160	130		220	240
18	210	120	120		120	320	150	200	210		220	100
19	200	0	140		50	50	320	0	160		250	140
20	220	70	120	140	10		320	170			70	240
21	220	70	50	160	330	0	320	220	220	70	220	220
22	220	70		290	330	220	0	0	0	70	210	120
23	100		60	270	0	340	210	130	320	90	220	230
24	220	0	0		330	220	190	0	0	220	320	230
25	110	240	70	240		340	0	220	320	0	240	180
26	140	0	110	60	320	10		170	0	0	80	180
27	90	0	90	20	50	0		220	0	0	270	140
28	210	290	90	160	70	220		0	220	0	270	140
29	150		80	150	70	0	140	0	70	210	220	220
30	0		70	240	0	220	220	90	0	220	240	0
31	0		220		0		220	220		230		240

Wind speed

Date	Jan	Feb	Mar	Apr	May	Jun	Jul	Aug	Sep	Oct	Nov	Dec
1	3,3	1,2	2,2	1,7	6,7	2,1	0,3	0,9	0,7	1,5	2,6	7,2
2	2,1	3,9	8,9	1,5	2,2	2,4	1	4,1	0,9	1,5	3,3	7,2
3	8,6	4,8	2,1	1,2	3,9	3,1	1,2	5,4	0,7	1,2	5,3	2,6
4	4,5	0,7	5,8	1	1,2	3,1	1	6,4	2,2	3,8	2,1	5,3
5	1	1,5	0,3	1,5	1,2	1,2	0,9	4,9	4,6	1,2	1,2	5,6
6	1,2	2,1	0,7	1,5	1,7	1,2	3,3	1,2	0	5	1	12,4
7	2,9	1	1,2	1,2	0,7	2,4	3,3	2,7	0,7	3,8	0,7	4
8	2,7	2,1	2,2	2,1	0,9	2,7	1,2	1,2	2,2	4,2	1,2	10,5
9	4,5	2,1	4,6	3,4	0,7	2,6	3,3	1,2	1,2	2	1,5	2,2
10	1,2	2,1	0,9	2,7	0	0,3	6	0,3	1,2	3,6	1,2	4,6
11	2,1	3,3	2,7	3,3	1,9	2,4	0,7	0,3	0,7	0,7	6,4	3,1
12	2,1	2,6	2,9	1,7	1,2	1,7	0,7	1,5	1,2	0,8	2,7	5,9
13	2,1	4,6	2,7	1,2	2,1	2,4	3,1	6,7	2,4	1	1,7	3,3
14	8,1	4	4,1	7	2,7	2,1	3,3	1	0,9	1,6	2,1	2,7
15	3,9	1,5	6,4	8,5	2,4	3,3	3,3	4,1	4,8	0,9	8,7	4,5
16	5,3	5,3	6,9	7,3	1,9	1,2	0,3	4,6	1,2	1,5	4,8	5,5
17	1,5	5,3	3,9	5,9	1,6	2,7	2,7	3,3	2,1	3,1	1,7	4,6
18	1,5	1	4,1	7,3	4,1	2,7	2,2	2,1	2,4	1	2,1	6,7
19	2,7	1,7	2,6	5,4	0,7	1,2	3,3	0	2,7	0,3	2,1	2,7
20	2,1	7,7	2,1	1,5	0,7	1,5	1,7	1,9	3	0,3	3,9	1
21	2,6	4,4	2,1	3,3	0,3	0	2,7	1,2	2,4	2,9	1,2	3,8
22	2,1	4,8	2,5	7,7	3,3	1,9	0,9	0,9	3,8	11,5	1,5	0,7
23	2,7	2,1	4,6	8,8	1,9	0,7	0,7	1	2,7	2,1	3,1	4
24	2,6	1,2	1,7	6,9	3,1	0,3	0,7	0,9	1,7	1,5	2,1	4,6
25	5,3	2,1	1,5	3,1	1,8	3,9	0,9	1,5	2,1	1,5	1	8,9
26	2,9	1,2	2,1	0,7	2,7	2,1	0,9	0,7	0,8	1,7	2,7	7,7
27	5,3	1,2	2,6	1,9	0,3	0	1,3	4	1,2	0,3	6,4	7
28	4,1	6,7	3,3	4,6	0,9	3,9	1,6	0,7	3,4	1,9	6	6
29	1,5		3,3	2,7	1,2	2,4	2,7	1,7	2,1	1	0,7	2,1
30	1,9		3,4	2,1	0,7	2,7	2,7	1,9	1,2	2,1	2,1	1,2
31	0,3		4,6		1,2		3,9	1,5		3,3		2,7

Attachment 4.2.

N/A represents days without wind data.

WINDSPEED	WIND DIRECTION																	
	0	10	20	30	50	60	70	80	90	100	110	120	130	140	150	160	170	180
0-1	7%	0%	0%	0%	1%	0%	1%	0%	0%	0%	0%	0%	0%	0%	0%	1%	0%	0%
1-2	7%	0%	0%	0%	1%	0%	1%	1%	1%	0%	0%	0%	0%	0%	0%	1%	1%	0%
2-3	0%	0%	0%	0%	1%	0%	1%	1%	1%	0%	1%	0%	1%	1%	1%	1%	1%	0%
3-4	1%	0%	0%	0%	0%	0%	1%	1%	0%	0%	0%	1%	0%	0%	0%	0%	1%	0%
4-5	0%	0%	0%	0%	0%	0%	1%	1%	0%	0%	0%	1%	0%	0%	1%	1%	0%	0%
5-6	0%	0%	0%	0%	0%	0%	1%	0%	1%	0%	0%	0%	0%	0%	0%	0%	0%	0%
6-7	0%	0%	0%	0%	0%	0%	1%	0%	0%	0%	0%	0%	0%	0%	0%	0%	0%	0%
7-8	0%	0%	0%	0%	0%	0%	0%	0%	0%	0%	0%	0%	0%	0%	0%	0%	0%	0%
8-9	0%	0%	0%	0%	0%	0%	0%	0%	0%	0%	0%	0%	0%	0%	0%	0%	0%	0%
10-11	0%	0%	0%	0%	0%	0%	0%	0%	0%	0%	0%	0%	0%	0%	0%	0%	0%	0%
11-12	0%	0%	0%	0%	0%	0%	0%	0%	0%	0%	0%	0%	0%	0%	0%	0%	0%	0%
12-13	0%	0%	0%	0%	0%	0%	0%	0%	0%	0%	0%	0%	0%	0%	0%	0%	0%	0%
Totalsum	15%	1%	1%	0%	2%	1%	8%	3%	4%	1%	1%	2%	1%	2%	2%	4%	1%	1%

WINDSPEED	WIND DIRECTION																Totalsum	
	190	200	210	220	230	240	250	260	270	290	300	310	320	330	340	360		N/A
0-1	0%	0%	0%	1%	0%	0%	0%	0%	0%	0%	0%	0%	0%	0%	1%	0%	2%	15%
1-2	0%	0%	1%	5%	1%	1%	0%	0%	0%	0%	0%	0%	1%	0%	1%	0%	2%	27%
2-3	0%	1%	1%	7%	1%	1%	0%	0%	0%	0%	1%	0%	3%	0%	0%	0%	1%	25%
3-4	0%	0%	0%	3%	1%	1%	0%	0%	0%	0%	0%	0%	1%	1%	1%	0%	1%	12%
4-5	0%	0%	0%	2%	1%	1%	0%	0%	0%	0%	0%	0%	0%	0%	0%	0%	1%	8%
5-6	0%	0%	0%	0%	0%	0%	0%	0%	0%	0%	0%	0%	0%	0%	0%	0%	1%	4%
6-7	0%	0%	0%	0%	0%	0%	0%	0%	1%	0%	0%	0%	0%	0%	0%	0%	1%	4%
7-8	0%	0%	0%	0%	0%	0%	0%	0%	0%	0%	0%	0%	0%	0%	0%	0%	1%	2%
8-9	0%	0%	0%	0%	0%	0%	0%	0%	1%	0%	0%	0%	0%	0%	0%	0%	0%	2%
10-11	0%	0%	0%	0%	0%	0%	0%	0%	0%	0%	0%	0%	0%	0%	0%	0%	0%	0%
11-12	0%	0%	0%	0%	0%	0%	0%	0%	0%	0%	0%	0%	0%	0%	0%	0%	0%	0%
12-13	0%	0%	0%	0%	0%	0%	0%	0%	0%	0%	0%	0%	0%	0%	0%	0%	0%	0%
Totalsum	1%	1%	2%	18%	3%	4%	0%	1%	2%	1%	2%	0%	4%	1%	4%	0%	9%	1

Attachment 5. Flettner rotor efficiency in kN

wind direction	wind speed	kN north	kN south	wind direction	wind speed	kN north	kN south
30	2,7	0,944	0,993	70	2,7	3,483	3,55
50	2,1	1,383	1,38	70	3,3	5,284	5,459
50	1,9	1,112	1,129	70	1,7	1,367	1,385
50	0,7	0,047	0,056	70	0,7	0,206	0,174
50	0,3	0	0	70	0,9	0,301	0,353
50	2,7	2,391	2,35	70	1,2	0,633	0,694
50	1,2	0,396	0,425	70	3,3	5,284	5,459
60	2,7	2,932	3,012	70	0,7	0,206	0,174
60	4,6	8,639	9,983	70	2,1	2,135	2,103
60	1	0,315	0,363	70	2,9	4,017	4,135
60	0,7	0,109	0,132	70	11,5	54,822	65,54
60	10,5	41,338	54,098	70	3,9	7,397	7,981
70	2,7	3,483	3,55	80	3,9	8,215	8,551
70	4,5	9,985	10,825	80	1,5	1,223	1,157
70	8,1	32,663	36,567	80	4,1	9,123	9,605
70	5,3	13,982	15,18	80	3,3	5,797	5,941
70	0,7	0,206	0,174	80	1,5	1,223	1,157
70	5,3	13,982	15,18	80	1,2	0,734	0,742
70	7,7	29,853	32,879	80	4,1	9,123	9,605
70	4,4	9,535	10,234	80	3,3	5,797	5,941
70	4,8	11,362	12,321	80	2,7	3,895	3,882
70	4,6	10,444	11,332	80	2,2	2,526	2,536
70	2,7	3,483	3,55	90	1	0,509	0,509
70	6,4	20,73	22,378	90	5,3	16,824	16,824
70	6,9	24,175	26,152	90	2,6	3,707	3,707
70	1,5	1,063	1,108	90	3,3	6,064	6,064
70	3,4	5,597	5,827	90	1,7	1,591	1,591
70	3,4	5,597	5,827	90	0,7	0,249	0,249

wind direction	wind speed	kN north	kN south
90	2,4	3,174	3,174
90	4,6	12,349	12,349
90	1,9	1,931	1,931
90	2,1	2,357	2,357
90	5,3	16,824	16,824
90	1,2	0,742	0,742
90	7,2	30,84	30,84
100	2,7	3,882	3,895
100	1,7	1,492	1,481
100	6,7	26,737	25,522
110	5,3	15,18	13,982
110	2,2	2,324	2,32
110	2,1	2,103	2,135
110	2,1	2,103	2,135
110	0,9	0,353	0,301
120	1	0,363	0,315
120	3,9	6,821	6,207
120	4,1	7,678	6,872
120	2,1	1,822	1,852
120	4,1	7,678	6,872
120	3,1	4,094	3,888
120	0,7	0,132	0,109
130	2,4	1,835	1,778
130	1	0,269	0,23
130	2,1	1,38	1,383
130	6,4	16,803	13,093
140	2,9	1,928	1,861
140	4	4,11	3,676

wind direction	wind speed	kN north	kN south
140	2,6	1,52	1,476
140	1,5	0,495	0,486
140	2,7	1,641	1,602
140	2,7	1,641	1,602
140	7	15,722	11,121
140	6	10,632	8,01
150	1,5	0,281	0,255
150	4,8	3,832	3,207
150	1,5	0,281	0,255
150	4,6	3,458	2,931
150	2,7	0,993	0,944
150	1	0,114	0
150	2,2	0,635	0,568
150	1,5	0,281	0,255

wind direction	wind speed	kN north	kN south	wind direction	wind speed	kN north	kN south
210	1,5	0,281	0,255	220	4,6	5,68	4,715
210	4,1	2,63	2,224	220	2,1	0,98	0,912
210	0,7	0	0	220	2,4	1,294	1,251
210	2,2	0,635	0,568	220	2,1	0,98	0,912
210	2,4	0,775	0,754	220	1,9	0,82	0,744
210	1	0,114	0	220	0,3	0	0
210	1,5	0,281	0,255	220	3,9	3,868	3,502
210	1,5	0,281	0,255	220	2,7	1,641	1,602
220	3,3	2,574	2,522	220	1,2	0,307	0,216
220	2,1	0,98	0,912	220	0,9	0,128	0,022
220	4,5	5,395	4,516	220	1,2	0,307	0,216
220	1,2	0,307	0,216	220	3,3	2,574	2,522
220	2,1	0,98	0,912	220	3,3	2,574	2,522
220	2,1	0,98	0,912	220	2,7	1,641	1,602
220	1,5	0,495	0,486	220	2,7	1,641	1,602
220	2,1	0,98	0,912	220	3,9	3,868	3,502
220	2,6	1,52	1,476	220	1,5	0,495	0,486
220	2,1	0,98	0,912	220	1,2	0,307	0,216
220	2,6	1,52	1,476	220	1,5	0,495	0,486
220	2,1	0,98	0,912	220	4	4,11	3,676
220	1	0,171	0,082	220	1,5	0,495	0,486
220	2,1	0,98	0,912	220	2,4	1,294	1,251
220	2,1	0,98	0,912	220	3,4	2,773	2,678
220	2,1	0,98	0,912	220	1,5	0,495	0,486
220	3,3	2,574	2,522	220	1,2	0,307	0,216
220	2,6	1,52	1,476	220	5	6,869	5,58
220	2,1	0,98	0,912	220	4,2	4,607	4,033
220	1,2	0,307	0,216	220	1,5	0,495	0,486

wind direction	wind speed	kN north	kN south	wind direction	wind speed	kN north	kN south
220	2,1	0,98	0,912	240	2,1	1,822	1,852
220	2,6	1,52	1,476	240	3,1	4,094	3,888
220	2,1	0,98	0,912	240	2,1	1,822	1,852
220	1	0,171	0,082	240	3,3	4,682	4,419
220	2,7	1,641	1,602	240	1,7	1,168	1,12
220	1,7	0,669	0,624	240	4,8	10,993	9,442
220	2,1	0,98	0,912	240	1	0,363	0,315
220	1,2	0,307	0,216	240	2,1	1,822	1,852
220	3,1	2,234	2,219	240	5,9	16,923	14,576
220	0,7	0,038	0	240	4,6	9,983	8,639
220	2,6	1,52	1,476	240	1	0,363	0,315
220	4,6	5,68	4,715	240	2,7	3,012	2,932
220	3,3	2,574	2,522	250	2,1	2,103	2,135
220	4,5	5,395	4,516	260	1,2	0,742	0,734
220	3,8	3,63	3,209	260	5,3	16,539	15,865
220	2,1	0,98	0,912	270	8,6	42,386	42,386
230	6,7	18,727	14,355	270	8,9	44,986	44,986
230	2,2	1,51	1,523	270	8,8	44,371	44,371
230	1,2	0,425	0,396	270	3,1	5,301	5,301
230	3,3	3,695	3,441	270	6,4	24,731	24,731
230	3,3	3,695	3,441	270	6	21,665	21,665
230	1,2	0,425	0,396	290	6,7	22,757	24,556
230	8,7	32,254	24,522	290	7,7	29,853	32,879
230	4	5,8	5,096	290	2,4	2,724	2,772
230	2,7	2,35	2,391	290	0,3	0	0
230	4	5,8	5,096	300	2,1	1,852	1,822
230	4,6	7,945	6,831	300	3,1	3,888	4,094
240	2,9	3,526	3,385	300	2,7	2,932	3,012

wind direction	wind speed	kN north	kN south
300	2,6	2,728	2,773
300	1,2	0,537	0,58
300	0,7	0,109	0,132
300	7,2	21,875	25,174
310	0,9	0,166	0,199
320	2,2	1	1,058
320	2,9	1,861	1,928
320	2,7	1,602	1,641
320	3,1	2,219	2,234
320	1,7	0,624	0,669
320	2,7	1,602	1,641
320	6	8,01	10,632
320	3,3	2,522	2,574
320	1,7	0,624	0,669
320	2,7	1,602	1,641
320	2,7	1,602	1,641
320	2,4	1,251	1,294
320	2,7	1,602	1,641
320	2,1	0,912	0,98
320	2,1	0,912	0,98
330	0,3	0	0
330	3,3	1,316	1,537
330	3,1	1,202	1,325
330	1	0	0,114

kN north total	kN south total	kN total
1213,742	1219,996	2433,738

Attachment 6. Lavik – Oppedal timetable.

E39 Lavik – Oppedal



Lavik - Oppedal			RUTE NR. 1046		
A: M/F «Oppedal»	120 bilar/cars - 350 Pass. } 916 81 170	B: M/F «Ampere»	120 bilar/cars - 350 Pass. } 916 81 179	C: M/F «Stavanger»	120 bilar/cars - 350 Pass. } 950 87 575

Overfartstid/Crossing time: cirka/approx. 20 min. Takstzone/ Farezone 6

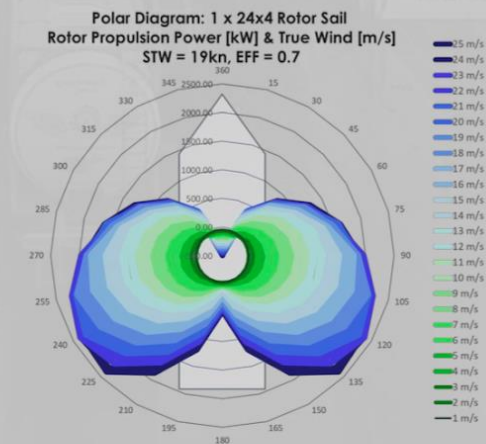
Frå Oppedal	Frå Lavik	Frå Oppedal	Frå Lavik	Frå Oppedal	Frå Lavik	Frå Oppedal	Frå Lavik	Frå Oppedal	Frå Lavik	Frå Oppedal	Frå Lavik
MÅNDAG - FREDAG						LAURDAG			SUNDAG		
A 0000	A 0030	A 0000	A 0030	A 0000	A 0030						
A 0100	A 0130	A 0100	A 0230	A 0100	A 0230						
A 0200	A 0230	A 0300	A 0430	A 0300	A 0430						
A 0300	A 0330	A 0500	A 0530	A 0500	A 0530						
A 0400	A 0430	B 0600	B 0630	A 0600	A 0630						
A 0500	A 0530	B 0700	B 0730	B 0700	B 0730						
B 0600	B 0630	A 0800	A 0830	B 0800	B 0830						
A 0700	A 0730	B 0830	B 0900	A 0900	A 0930						
B 0730	B 0800	A 0900	A 0930	B 0930	B 1000						
A 0800	A 0830	B 0930	B 1000	A 1000	A 1030						
B 0830	B 0900	A 1000	A 1030	B 1030	C 1050						
A 0900	A 0930	B 1030	B 1100	A 1100	B 1110						
B 0930	C 0950	A 1100	A 1130	C 1120	A 1130						
A 1000	B 1010	B 1130	B 1200	B 1140	C 1150						
C 1020	A 1030	A 1200	A 1230	A 1200	B 1210						
B 1040	C 1050	B 1230	B 1300	C 1220	A 1230						
A 1100	B 1110	A 1300	A 1330	B 1240	C 1250						
C 1120	A 1130	B 1330	B 1400	A 1300	B 1310						
B 1140	C 1150	A 1400	A 1430	C 1320	A 1330						
A 1200	B 1210	B 1430	B 1500	B 1340	C 1350						
C 1220	A 1230	A 1500	A 1530	A 1400	B 1410						
B 1240	C 1250	B 1530	B 1600	C 1420	A 1430						
A 1300	B 1310	A 1600	A 1630	B 1440	C 1450						
C 1320	A 1330	B 1630	B 1700	A 1500	B 1510						
B 1340	C 1350	A 1700	A 1730	C 1520	A 1530						
A 1400	B 1410	B 1730	B 1800	B 1540	C 1550						
C 1420	A 1430	A 1800	A 1830	A 1600	B 1610						
MÅNDAG - FREDAG						LAURDAG			SUNDAG		
B 1440	C 1450	B 1830	B 1900	C 1620	A 1630						
A 1500	B 1510	A 1900	A 1930	B 1640	C 1650						
C 1520	A 1530	B 1930	B 2000	A 1700	B 1710						
B 1540	C 1550	A 2000	A 2030	C 1720	A 1730						
A 1600	B 1610	B 2030	B 2100	B 1740	C 1750						
C 1620	A 1630	A 2100	A 2130	A 1800	B 1810						
B 1640	C 1650	A 2200	A 2230	C 1820	A 1830						
A 1700	B 1710	A 2300	A 2330	B 1840	C 1850						
C 1720	A 1730			A 1900	B 1910						
B 1740	C 1750			C 1920	A 1930						
A 1800	B 1810			B 1940	C 1950						
C 1820	A 1830			A 2000	B 2010						
B 1840	C 1850			C 2020	A 2030						
A 1900	B 1910			B 2040	C 2050						
C 1920	A 1930			A 2100	B 2110						
B 1940	C 1950			C 2120	A 2130						
A 2000	B 2010			B 2140	B 2210						
C 2020	A 2030			A 2200	A 2230						
B 2040	C 2050			B 2240	B 2310						
A 2100	B 2110			A 2300	A 2330						
C 2120	A 2130										
B 2140	B 2210										
A 2200	A 2230										
B 2240	B 2310										
A 2300	A 2330										

Attachment 7. Specification sheet provided by Norsepower

(Published by approval form Norsepower)

Technical specifications

Model	18 x 3	24 x 4	30 x 5
Rotor			
Rotor height x diameter [m]	18 x 3	24 x 4	30 x 5
Material	GFRP/CFRP sandwich	GFRP/CFRP sandwich	GFRP/CFRP sandwich
Rotor speed [rpm]	0-250, variable	0-225, variable	0-180, variable
Lightning conductor / Ice prevention	Yes / Optional	Yes / Optional	Yes / Optional
Support structure			
Tower	Cylindrical/conical steel structure	Cylindrical/conical steel structure	Cylindrical/conical steel structure
Foundation height (typical) [m]	2	2.5	3
Weight of typical foundation [tons]	9	13	17
Rotor Sail assembly weight without foundation [tons]	20	27	42
Drive			
Electric motor	55 kW, 50/60 Hz IE4, IP55	90 kW, 50/60 Hz IE4, IP55	110 kW, 50/60 Hz IE4, IP55
Variable speed drive	ABB, Siemens or similar (400/440V)	ABB, Siemens or similar (400/440V)	ABB, Siemens or similar (400/440V)
Brake resistor / Mechanical lock	Yes / Optional	Yes / Optional	Yes / Optional
Control system software	NorseControl	NorseControl	NorseControl
Hardware	Beckhoff/Siemens/similar automation, distributed system	Beckhoff/Siemens/similar automation, distributed system	Beckhoff/Siemens/similar automation, distributed system
Condition Monitoring System	Yes	Yes	Yes
Hydraulic Tilting mechanism	Optional	Optional	Optional
ATEX compliant design	Optional	Optional	Optional
Ambient conditions			
Operational temperature	+50 – (-30)C	+50 – (-30)C	+50 – (-30)C
Operational wind speed range	0-25 m/s	0-25 m/s	0-25 m/s
Survival wind speed	70 m/s	70 m/s	70 m/s
Thrust (max. continuous)	100 kN (limited)	175 kN (limited)	270 kN (limited)



At Norsepower we work continuously to develop and further improve our system, so we reserve the right to make changes to the information presented in this brochure without notice.

www.norsepower.com